Dynamic Structure Factor of Diblock Copolymers in the Ordering Regime

6 AUTHORS, INCLUDING:

Spiros H. Anastasiadis
Foundation for Research and Technology - H…

176 PUBLICATIONS   **4,563** CITATIONS

SEE PROFILE

Dynamic Structure Factor of Diblock Copolymers in the Ordering Regime

A. N. Semenov*

University of Leeds, Department of Applied Mathematics, Leeds LS2 9JT, U.K., and Nesmeyanov Institute of Organo-Element Compounds of Russian Academy of Science, 28 Vavilova St., Moscow 117812, Russia

S. H. Anastasiadis,*,† N. Boudenne,‡ and G. Fytas

Foundation for Research and Technology−Hellas, Institute of Electronic Structure and Laser, P.O. Box 1527, 711 10 Heraklion Crete, Greece

M. Xenidou and N. Hadjichristidis§

Department of Chemistry, University of Athens, 157 01 Zografou Athens, Greece

Received May 16, 1997; Revised Manuscript Received August 1, 1997[⊗]

ABSTRACT: The modes of relaxation of composition fluctuations in disordered diblock copolymer systems have been experimentally and theoretically investigated for wavevectors q near the maximum of the static structure factor, q_c. By use of disordered semidilute solutions of a very high molecular weight diblock in a nonselective good solvent, the dynamic structure factor $S(q,t)$ is probed in this q range by photon correlation spectroscopy over a broad time range. Two relaxation processes are observed to contribute to $S(q,t)$ besides the cooperative diffusive relaxation of the total polymer concentration fluctuations: the well-anticipated internal copolymer relaxation, which is a single exponential process near q_c and for which the effect of the proximity to the disorder-to-order transition (ODT) is evident both in the respective static light scattering intensity and in the relaxational dynamics by increasing the copolymer concentration in the range $\phi^* < \phi < \phi_{ODT}$; and an extra relaxation, faster than the internal, which is less influenced by the thermodynamics. A general theory for the dynamic structure factor for entangled diblock copolymer systems is presented which adequately describes the internal relaxation within the reptation model and predicts the existence of another relaxation mechanism due to Rouse-like motions related to curvilinear chain fluctuations inside their tubes. The theory can semiquantitatively account for the combined characteristics of the two processes.

I. Introduction

The relative motion of polymeric chains in multiconstituent polymer systems, i.e., the main channel for relaxation of the most probable composition fluctuations, is controlled by the thermodynamic interactions between the dissimilar components and their mobilities. For binary polymer blends, the relative motion of one species with respect to the other results is the well-known interdiffusion process; a thermodynamic slowing down of the mutual diffusion coefficient near the macrophase separation has been well documented.[1] For diblock copolymers, consisting of two covalently bonded linear sequences of chemically distinct species A and B, the relaxation of the order parameter fluctuations proceeds via the collective relative motion of one block with respect to the other resulting in the internal copolymer mode.[2,3] According to the dynamic random-phase-approximation (RPA), this is the only mechanism for the relaxation of composition fluctuations in an incompressible, monodisperse diblock copolymer melt in the disordered state.[3] In the low wavevector (q) limit, the characteristic thermal decay rate of the internal process, being purely kinetic, is determined by the

longest (internal) conformational chain relaxation time; i.e., the effects of the thermodynamic interactions are negligible. This process has been investigated by probing the relaxation of composition fluctuations in homogeneous disordered systems in the melt[4] and/or in solutions[5−8] in a common good solvent by dynamic light scattering[4,6−8] and/or neutron spin−echo.[5] For solutions, the dynamics of total concentration fluctuations relax via another fast diffusive process, i.e., via the cooperative diffusion of the transient network of the overlapping polymer chains,[3,6−8] similarly to semidilute homopolymer solutions. Besides, an additional diffusive relaxation (the so-called "polydispersity" or "heterogeneity" diffusive mode) has been observed by photon correlation spectroscopy (PCS) at low wavevectors both in disordered melts[4] and solutions,[6,8] which has been identified[6,9,10] with the copolymer self-diffusivity observable due to the small but finite inherent composition polydispersity of the diblock. Recent reviews[11] provide an extensive account on the research work on block copolymer dynamics.

The disorder-to-order transition[12] (ODT) for diblock copolymers[13] of a certain composition f (volume fraction of component A) is controlled by χN, where N is the total number of links and χ the Flory−Huggins interaction parameter between A and B links; it leads from a homogeneous or disordered state at low enough values of χN toward a microphase separated state characterized by long range order in its composition at higher χN values. In diblock copolymer solutions in good solvents, the unfavorable interactions between the blocks are diluted by the solvent and the ODT is more easily accessed even for copolymers with high N.[14,15] In

semidilute solutions, χN is renormalized[6,14c] as $\chi^* N \propto \chi N \phi^{(1-z)/(3\nu-1)} \cong \chi N \phi^{1.59}$, with ν the Flory exponent ($\nu = 0.59$ in good solvents) and $z = -0.225$. Below, we discuss semidilute entangled solutions of nearly symmetric diblocks with large N, $N/N_e(\phi) > 1$; $N_e(\phi)$ is the mean number of links between entanglements along the chain at concentration ϕ.

In a recent paper,[16] the dynamics of the order parameter fluctuations in disordered diblock copolymer solutions near the maximum of the static structure factor, $S(q)$, were addressed in the proximity to the disorder-to-order transition (ODT). The main aim was to assess the thermodynamic effects on the internal copolymer process, and hence, measurements were necessary near the maximum of $S(q)$. Extending that work,[16] we present in this paper a thorough theoretical and experimental study of the intermediate scattering function $S(q,t)$ for disordered diblock copolymer solutions near ODT for $qR_g \approx O(1)$ (R_g being the radius of gyration) and over a wide time range (10^{-6}–10^3 s). The synthesis of a very high molecular weight (MW) diblock copolymer was crucial for the experimental part of the present study; the very high MW was needed in order to place $q_c \sim O(1/R_g)$, at which $S(q)$ attains its maximum, in the light scattering q range. In order to investigate the disordered state, semidilute solutions in a neutral good solvent are used. The observed relaxation processes are (i) the cooperative diffusion which is identical to semidilute homopolymer solutions, (ii) the internal copolymer mode which shows clear evidence of the effects of the proximity to ODT in both the static light scattering intensity and the relaxational dynamics as the copolymer concentration is increased in order to approach the ordered state, i.e., a slowing down of its relaxation rate that accompanies the significant increase of the static intensity, and (iii) an extra relaxation, faster and weaker than the internal, that appears when the solution enters the entanglement regime, which is much less influenced by the thermodynamics. On the theoretical side, we present a general theory for the calculation of the $S(q,t)$ for entangled diblock copolymer solutions using the RPA approach and the classical reptation model.[17–19] A detailed comparison between the theoretical and experimental $S(q,t)$ identifies two mechanisms for the relaxation of the order parameter fluctuations, which relate to the slower reptation relaxation internal mode and to a new faster mode due to Rouse-like chain fluctuations inside the "fixed" reptation tube; the refractive index contrast and the large N make this Rouse process visible; the effects of thermodynamics for the Rouse process are less important. Careful shape analysis of the $S(q,t)$ reveals the exponentiality of the microdomain scale ($\sim 1/q_c$) composition fluctuations near ODT. Theory quantitatively accounts for the combined characteristics of the two processes; the polydispersity mode is not observed by PCS due to the dominating intensity of the internal process.

This article is arranged as follows: The complete theory for the relaxation of composition fluctuations is presented in section II. Following the Experimental Section III, the detailed analysis of the experimental intermediate scattering functions is presented in section IV, and the results are discussed in relation to the theory in section V. Finally, the concluding remarks constitute section VI.

II. Theoretical Approach

II.1. Pure Reptational Relaxation Mode. For simplicity in the paper, we consider a symmetric ($N_A = N_B$) diblock copolymer system consisting of geometrically similar blocks (same statistical segment, b, and volume per link, v) with long enough chains, so that the system is entangled, $N = N_A + N_B \gg N_e$. One can distinguish two basic types of concentration fluctuations: (i) fluctuations of total concentration $\phi = \phi_A + \phi_B$ and (ii) composition fluctuations characterized by the order parameter $\eta = (\phi_A - \phi_B)/2$, where ϕ_A and ϕ_B are the volume concentrations of A and B links. Fluctuations of the total polymer concentration in diblock copolymers can be described[6] in exactly the same way as for the analogous homopolymer systems; the amplitude of these fluctuations is inversely proportional to the solution osmotic pressure and their diffusive (q^2-dependent) thermal decay rate defines the cooperative diffusion coefficient in the solution. The amplitude of fluctuations of total concentration is usually negligible in experimentally interesting regimes (see below) in comparison to that of composition fluctuations, which is the focus on the present work. The latter define the intermediate scattering function or dynamic structure factor

$$S(q,t) = \frac{1}{v}\langle \eta_q(t)\eta_{-q}(0)\rangle \tag{1}$$

where $\eta_q(t) = \int \eta(\mathbf{r},t) \exp(i\,\mathbf{qr})\,\mathrm{d}^3 r$, with $i^2 = -1$.

The dynamic structure factor for block copolymer melts and solutions has been theoretically considered before[3] using the dynamic RPA[20] approach; however, in all those publications the Rouse dynamics (with no entanglements) was considered. Relaxations of composition fluctuations for *entangled* block copolymer melts (as well as for entangled homopolymer blends) were investigated before[2] using the fluctuation dissipation theorem,[21] the dynamic RPA,[22] and the reptation model.[19] Taking into account that experimental data become now available and that the original publication[2] is, in some part, not detailed enough, a rather detailed consideration of the entangled block copolymer in the melt case following the main ideas of ref 2 is presented in the Appendix.

A general expression for the Laplace transform of the generalized susceptibility $\kappa(q,p) = \int_0^\infty \kappa(q,t)e^{-pt}\,\mathrm{d}t$ has been obtained[2] as

$$\kappa(q,p) = \frac{N\phi_0}{F(u,\sigma) - 2\chi N} \tag{2}$$

where q is the wavevector, p is the Laplace variable, $\phi_o = 1$ is the polymer volume fraction, $F(u,\sigma) = 4(u^2 - \sigma^2)/[\Psi(u,\sigma) - \Psi(u,u)]$, $\sigma \equiv (pt^*)^{1/2}$, $u \equiv q^2 R_g^2/2$, $R_g = \alpha N^{1/2}$ is the radius of gyration of the chain, $\alpha = b/6^{1/2}$ with b the statistical segment length, $\Psi(u,\sigma) = \{2(u^2/\sigma)[1 - 1/\cosh \sigma] - \sigma\}/[\sigma + u \tanh \sigma]$, and

$$t^* = \frac{N^2}{4D^*} = \frac{\tau_0}{4}\frac{N^3}{N_e} \tag{3}$$

with $D^* = TN_e/(N\zeta_0/b^2)$ the Rouse diffusivity along the reptation tube,[19] N_e the characteristic number of segments for entanglements, and $\tau_0 = \zeta_0 b^2/T$ the microscopic time with ζ_0 the friction coefficient per link.

The dynamic structure factor for pure reptational motion is then represented as a superposition of relaxation modes:

$$S_{\mathrm{rept}}(q,t) = \sum_k I_k(q) \exp[-\Gamma_k(q)\,t] \tag{4}$$

where the set of relaxation rates, $\Gamma_k(q)$, and the intensities, $I_k(q)$, can be calculated from

$$1/\kappa(q,-\Gamma_k) = 0; \qquad I_k = \frac{1}{\Gamma_k}\,\mathrm{Res}_{p=-\Gamma_k}[\kappa(q,p)] \quad (5)$$

where Res means the residue of a pole singularity.

Generalization of the above treatment for the case of block copolymer solutions is straightforward. The basic eqs 2 and 4 hold also for a solution in exactly the same form as for a melt with the only difference being that now $\phi = \phi_o < 1$. Besides, a renormalization of the basic parameters has to be taken care, i.e., of the typical reptation time t^*, the radius of gyration R_g, and the effective interaction parameter χ. For a good solvent, these renormalizations are easily done using the blob concept.[17] The solution can be considered as a quasimelt of blobs with $g \cong \phi^{-1/(3\nu-1)}$ links per blob, where $\nu \cong 0.59$ is the Flory exponent. Thus, the following substitutions in the above equations are $\alpha \to \xi$, $N \to N/g$, $\tau_0 \to \tau_g \cong \tau_0(\xi/\alpha)^3 \cong \tau_0\phi^{-3\nu/(3\nu-1)}$, $N_e \to N_e^* = N_e(\phi)/g$ (N_e^* slightly decreases as concentration decreases[23]). The scattering function should also be multiplied by the factor g since each unit (blob) now consists of g scatterers. Here, ξ is the typical blob size, $\xi \cong bg^\nu \cong b\phi^{-\nu/(3\nu-1)}$, and τ_g the Zimm relaxation time of one blob. Hence,

$$R_g \cong \alpha N^{0.5}\phi^{-(\nu-0.5)/(3\nu-1)}$$

$$\tau^* \cong \frac{1}{4}\tau_0\,\frac{N^3}{N_e(\phi)}\,\phi^{(2-3\nu)/(3\nu-1)} \quad (6)$$

The renormalization of the interaction parameter is less trivial and has been considered previously;[24,25,14c,6] the χ parameter is appreciably screened by the presence of good solvent,

$$\chi^* = \chi\phi^{(1-z)/(3\nu-1)} \quad (7)$$

where $z \cong -0.225$ and χ is the priming interaction parameter characterizing a blend of A and B polymers.

Since in Leibler's mean-field approximation, the critical point corresponding to the ODT is predicted[12] at $\chi_c^*N \cong 10.5$ and $q_cR_g \cong 1.95$, where q_c is the critical scattering vector, the solution should exhibit a critical concentration for ODT at

$$\phi_c \cong [10.5/(\chi N)]^{(3\nu-1)/(1-z)} \quad (8)$$

Taking into account all the renormalizations, the generalized susceptibility of the solution is obtained in a form which is identical to eq 2 with the substitution $\chi \to \chi^*$, whereas $S_{\mathrm{rept}}(q,t)$ is also represented by eq 4.

The dynamics of composition fluctuations for arbitrary q values can be characterized by the initial relaxation rate, $\Omega(q) = -\mathrm{d}\ln S(q,t)/\mathrm{d}t|_{t=0} = \sum_k I_k(q)\Gamma_k(q)/\sum_k I_k(q)$, and by the mean relaxation time,[3] $T(q) = -\int t(\partial S(q,t)/\partial t)(\mathrm{d}t/S(q,0)) = \sum_k I_k(q)\tau_k(q)/\sum_k I_k(q)$, where $I_k(q)$ and $\Gamma_k(q)$ are defined in eq 5, and $\tau_k(q) = 1/\Gamma_k(q)$ is the relaxation time of the kth mode. The quantity $[\Omega(q)-T(q) - 1]$ is a measure of the deviation from a single exponential shape; for a single exponential decay, this nonexponentiality parameter is obviously exactly equal to zero while for a nonexponential relaxation it is strictly

positive. Both $\Omega(q)$ and $T(q)$ can be directly calculated using eq 4

$$\Omega(q) = \frac{1}{8t^*}[F(u,0) - 2\chi^*N](3 - 4e^{-u} + e^{-2u}) \quad (9a)$$

$$T(q) = \frac{t^*}{u^2}\frac{F(u,0)}{F(u,0) - 2\chi^*N}\left[\frac{uF(u,0)}{12}\frac{1 + u/4}{1 + u} - 1\right] \quad (9b)$$

The above equations imply the following asymptotic behavior of the mean relaxation rate

$$\Omega(q) = \begin{cases} 3/t^* & \text{for } u \ll 1 \\ 1.5u/t^* & \text{for } u \gg 1 \end{cases} \quad (9c)$$

and of the mean relaxation time

$$T(q) = \begin{cases} 0.4t^* & \text{for } u \ll 1 \\ t^*/12 & \text{for } u \gg 1 \end{cases} \quad (9d)$$

Note that the mean relaxation time is always of the order of the reptation (disentanglement) time of the whole block copolymer chain, t^*. The relaxation is nearly exponential in the region of small wavevectors, where $[\Omega(q)T(q) - 1] \cong 0.2$ for $u \ll 1$; however, it becomes exceedingly nonexponential for shorter wavelengths, $[\Omega(q)T(q) - 1] \cong u/8$ for $u \gg 1$. Yet, near the critical wavevector $q_c \cong 1.95/R_g$, at which $S(q)$ attains its maximum value, the deviations from a single exponential representation of $S(q,t)$ are still small: $[\Omega(q_c)T(q_c) - 1] = 0.22$; i.e., the higher-order modes are not important near q_c. Note that, according to eqs 9, the nonexponentiality parameter does not depend on the χ^* parameter.

The asymptotic behavior of the solution dynamic structure factor in the region $qR_g \ll 1$ is relevant with respect to experiments with low MW diblock copolymers. For $qR_g \ll 1$,

$$S_{\mathrm{rept}}(q,t) =$$

$$\phi Nq^2R_g^2\frac{4}{\pi^4}\sum_k\frac{1}{(2k+1)^4}\exp\left[-\frac{\pi^2(2k+1)^2}{4}\frac{t}{t^*}\right] \quad (10)$$

which does not depend on the χ^* parameter in this region; k is a positive integer or 0. The relaxation rate and the intensity of the main mode ($k = 0$) are

$$\Gamma_0 = \pi^2/(4t^*); \qquad I_0 = (4/\pi^4)\phi Nq^2R_g^2 \quad (11)$$

Note that the first higher-order mode ($k = 1$) is 9 times faster and $3^4 = 81$ times weaker than that of the main mode ($k = 0$). The ratio I_1/I_0 becomes even smaller than $1/81$ in the vicinity of the ODT (numerical calculations show that, in the region $q/q_c \cong 0.5-1$, $\phi/\phi_c \cong 0.5-1$, where most of the measurements reported in the Experimental Section were performed, the ratio I_1/I_0 is smaller than $1/100$). Therefore, it is hardly possible that the higher-order reptation modes could be observed experimentally.

II.2. Reptation and Tube-Length Fluctuations: The Rouse Mode. In the preceding section, $S(q,t)$ was derived based on the pure reptation theory, in which all monomers of a chain are moving with the same velocity along the tube axis. However, even in the deeply entangled regime, the conformational dynamics of polymer chains is always a combination of reptation and Rouse-like motions. In the region $qR_g \lesssim 1$, the most important Rouse motions relate to chain conformational fluctuations inside the tube, i.e., fluctuations of the

curvilinear distance between any two monomers. The corresponding Rouse relaxation of a reptating chain was considered by de Gennes[26] for the case of a homopolymer system and for $qR_g \gg 1$. In this section, the theory is extended to include the case of block copolymers and consider also the regime $qR_g \lesssim 1$.

Prior to the quantitative approach, we present first the basic physical picture leading to the characteristic features of the dynamic structure factor due to Rouse-like motions, $S_R(q,t)$. In a thought experiment, it is assumed that a weak external field, for example $U^{ext}(\mathbf{r},t) = -\epsilon \sin(qy)H(t)$, is applied to the ideal block copolymer system (with no excluded volume or χ interactions) at $t = 0$; y is one Cartesian axis and $H(t)$ is the Heaviside function. Using eq A.1 in the Appendix, that relates the average linear response of a system to an external perturbation field to the susceptibility, the time-dependent order-parameter, $\eta(\mathbf{r},t) = \eta_q(t)\sin(qy)$, induced by the field, is directly related to the scattering function

$$\eta_q(t) = [S(q) - S(q,t)]\epsilon/T \qquad (12)$$

Since U^{ext} is actually the difference $U_A^{ext} - U_B^{ext}$, it is assumed without any loss of generality that $U_A^{ext} = -U_B^{ext} = -\epsilon \sin(qy)H(t)/2$. The two blocks of a particular chain are influenced by this field (for simplicity, only the case $qR_g \ll 1$ is considered here), subjected to two opposite external forces, $f_A = -(N/2)(\partial U_A^{ext}/\partial y) = Nq\epsilon \cos(qy)/4$ and $f_B = -(N/2)(\partial U_B^{ext}/\partial y) = -f_A$; assuming for simplicity that the chain is located near the origin at $y = 0$, $f_A = Nq\epsilon/4 \equiv f$, and $f_B = -f$. Obviously, these two forces will induce a "polarization" $\mathbf{P}$ of the chain in the y-direction via a shifting of the centers of mass of two blocks in opposite directions; the vector $\mathbf{P}$ connects the centers of mass.

Two basic mechanisms of this polarization can be distinguished: (i) due to changes of the tube conformation and (ii) due to additional elongation or compression of parts of the flexible chain along the fixed tube. The characteristic time and intensity associated with the first process (=reptation) were given in eq 11. The second process corresponds to one-dimensional (curvilinear) Rouse motion of the topological blobs along the tube. Therefore, the longest relaxation time associated with the second process is the Rouse time of a linear chain of $n_e = N/N_e(\phi)$ topological blobs (entanglements), i.e., $\tau_R \sim \tau_e n_e^2$, where $\tau_e = \tau_g(N_e^*)^2$ is the Rouse-Zimm relaxation time of one topological blob, and, hence

$$\tau_R = \frac{1}{3\pi^2}\tau_0\phi^{(2-3\nu)/(3\nu-1)}N^2 \qquad (13a)$$

which is clearly shorter than t^* (eq 6).

As for an electrostatic system, the order parameter η (which is analogous to "charge") must be proportional to the divergence of polarization: $\eta \sim \phi \, \mathrm{div} \, \mathbf{P} \sim \phi q \mathbf{P}$. An estimate is now made for the polarization, P, associated with the two mechanisms mentioned above. For times of $O(t^*)$, the equilibrium polarization can be found by balancing the decrease in potential energy of the chain, Pf, and the corresponding elastic energy, $F_{el} \sim TP^2/R_g^2$; thus, $P \sim R_g^2 f/T$. Using eq 12, one can obtain the intensity of the reptation mode as $I_{rept} \sim \eta T/\epsilon \sim \phi Nq^2R_g^2$, which is, in fact, in agreement with eq 11. Alternatively, on a shorter time-scale, of $O(\tau_R)$, the tube conformation is nearly fixed, and, therefore, the intensity of the Rouse mode is connected to the polarization P_R induced by the external force in a nearly fixed tube, i.e., by stretching the two blocks along the tube on some length ΔL; then $P_R \sim (\Delta L/L_t)R_g$. Balancing the corre-

sponding elastic energy, $F_{el} \sim Tn_e(\Delta L/L_t)^2 = T(\Delta L)^2/R_g^2$, with the potential energy $P_R f$, one gets $P_R \sim R_g^2(f/T)-(R_g^2/L_t^2) \sim R_g^2(f/T)/n_e$. Thus, the intensity of the Rouse mode is

$$I_R \sim \phi q^2 R_g^2 N_e(\phi) \qquad (13b)$$

Note that the ratio of the intensities of the two modes is of order of the number of entanglements per chain: $I_{rept}/I_R \sim n_e$, similar to the ratio of the corresponding relaxation times (eqs 11 and 13), $\tau_{rept}/\tau_R \sim t^*/\tau_R \sim n_e$.

The effect of χ-parameter on the Rouse mode should be much weaker than for the longer scale reptation motion (eq 9) based on the following arguments. The molecular field associated with the χ^* parameter is $U^{mol} = -2\chi^* T\eta/\phi$, where the highest possible value of χ^* in the disordered state is $\chi_c^* \sim 1/N$. Since the typical composition fluctuation that develops during the Rouse stage, is $\eta \sim I_R\epsilon/T$, the upper boundary for the molecular field is $U^{mol} = \epsilon/n_e$. Therefore, during the Rouse stage the molecular field can be neglected in comparison with the external field of $O(\epsilon)$, so that the results obtained for the athermal ($\chi = 0$) case are more generally valid; in this regime ($t \sim \tau_R$, $p \sim 1/\tau_R$, $n_e \gg 1$) the relaxation characteristics of the interactive system and of the corresponding ideal system must nearly coincide.

Toward a quantitative derivation of the intermediate scattering function $S_R(q,t)$ corresponding to the curvilinear Rouse motion, the melt case is considered first ($\phi_0 = 1$). The dynamic structure factor can be obtained (eq 12) from the system response, $\eta_q(t)$, to weak external fields $U_A^{ext}(\mathbf{r},t) = -(\epsilon/2)\exp(-i\,\mathbf{qr})H(t)$, $U_B^{ext}(\mathbf{r},t) = -U_A^{ext}(\mathbf{r},t)$. A block copolymer chain is considered, which is confined in a tube created by surrounding chains; the topological interactions (entanglements) are still present in the otherwise ideal system. The immediate response of the chain to the field on scales larger that the tube diameter, d_e, would be a shift of its segments along the tube: $s(n,t) = s(n) + x(n,t)$, where s is the coordinate along the tube axis. The corresponding field-induced order parameter related to this shift is

$$\eta_q(t) = (1/2)(\phi_0/N)\sum_n \langle \exp[-i\,\mathbf{qR}(s(n) + x(n,t))] -$$
$$\exp[-i\,\mathbf{qr}(s(n))]\rangle h(n) \quad (14a)$$

where the function $\mathbf{R}(s)$ specifies the tube axis, so that $\mathbf{R}(s(n))$ is the initial conformation of the chain. Assuming that the spatial displacement of a monomer $\Delta R = |\mathbf{R}(s(n) + x(n,t)) - \mathbf{R}(s(n))| \sim (x(n,t)/L_t)^{1/2}R_g$ is small compared to the wavelength $1/q$ (this assumption is verified below), $\eta_q(t)$ is rewritten as[27]

$$\eta_q(t) = \frac{1}{2}\frac{\phi_0}{N}\sum_n h(n)\frac{\mathrm{d}n}{\mathrm{d}s}\Big\langle x(n,t)\frac{\partial}{\partial n}\exp[i\,\mathbf{qr}(n)]\Big\rangle \quad (14b)$$

where $\mathrm{d}n/\mathrm{d}s = N/L_t$ is the averaged one-dimensional density of the chain along the tube. The master Rouse equation which governs the one-dimensional dynamics of the chain in the tube can be written as

$$\zeta_0 \frac{\partial x}{\partial t} = \frac{T}{2\alpha^2}\frac{\partial^2 x}{\partial n^2} + g(n,t) \qquad (15)$$

where

$$g(n,t) = -\frac{\partial U}{\partial s} = -\frac{\mathrm{d}n}{\mathrm{d}s}\frac{\partial U}{\partial n} = \frac{N}{L_t}h(n)\frac{\partial}{\partial n}\Big(\frac{\epsilon}{2}e^{i\,\mathbf{qr}(n)}\Big)H(t)$$

is the external force acting on the nth monomer. The solution of the Rouse equation, with boundary conditions $\partial x/\partial n = 0$ for $n = 0, N$, can be represented in the form

$$x(n,t) = \int K_{t-t'}(n,n') g(n',t') \, dn' \, dt' \qquad (16a)$$

with

$$K_t(n,n') = \frac{1}{N\zeta_0} \sum_l \cos\left(\frac{\pi l n}{N}\right) \cos\left(\frac{\pi l n'}{N}\right) \exp[-t l^2/\tau_R] \qquad (16b)$$

where $\tau_R = \tau_0 N^2/(3\pi^2)$ is the Rouse time, and $l = 0, \pm 1, \pm 2 \ldots$

Using eqs 14−16, the average order parameter is calculated as[28]

$$\eta_q(t) = \frac{\epsilon N_e \phi_0}{12\pi^2 T} \sum_l \frac{1 - \exp[-t l^2/\tau_R]}{l^2} \int\int dn \, dn' \, h(n) h(n') \times$$
$$\cos\left(\frac{\pi l n}{N}\right) \cos\left(\frac{\pi l n'}{N}\right) \frac{\partial}{\partial n} \frac{\partial}{\partial n'} \langle e^{i\mathbf{q}\mathbf{r}(n) - i\mathbf{q}\mathbf{r}(n')} \rangle$$

Assuming Gaussian statistics, $\langle e^{i\mathbf{q}\mathbf{r}(n) - i\mathbf{q}\mathbf{r}(n')} \rangle = \exp[-q^2\alpha^2|n - n'|]$ and using eq 12, one gets the contribution to the scattering function due to the one-dimensional Rouse-like motions:

$$S_R(q,t) = \frac{N_e \phi_0}{6\pi^2} \sum_l J_l \exp[-t l^2/\tau_R] \qquad (18a)$$

where

$$J_l = \frac{1}{l^2} \int\int dn \, dn' \, h(n) h(n') \cos\left(\frac{\pi l n}{N}\right) \times$$
$$\cos\left(\frac{\pi l n'}{N}\right) \frac{\partial}{\partial n} \frac{\partial}{\partial n'} \exp[-q^2\alpha^2|n - n'|] \quad (18b)$$

and l is now a positive integer, $l = 1, 2, \ldots$ The mode with $l = 0$ corresponds to a reptation of the chain as a whole along the tube (already considered in section II.1), whereas the fluctuations inside the tube give rise to a number of Rouse modes with usual relaxation times τ_R, $\tau_R/4$, $\tau_R/9$, ...

Evaluation of the integrals in eq 18b results in a rather complicated general expression for the reduced intensities

$$J_l = J_l(u) = \frac{2u}{l^2}\left[1 - \frac{4u M_l}{(4u^2 + \pi^2 l^2)^2}\right] \qquad (19)$$

with $u = q^2 R_g^2/2$ and

$$M_l = \begin{cases} (u+2)(4u^2 + \pi^2 l^2) - 12u^2 + 4u^2 e^{-2u} + \\ \qquad 8\pi u l e^{-u}(-1)^{(l+1)/2} \text{ if } l = \text{odd} \\ u(4u^2 + \pi^2 l^2) - 12u^2 - 4u^2 e^{-u} + \\ \qquad 16u^2 e^{-u}(-1)^{l/2} \text{ if } l = \text{even} \end{cases}$$

One may consider the Rouse relaxation in the two asymptotic limits $u \gg 1$ and $u \ll 1$. For $u \gg 1$,

$$J_l \cong \frac{2\pi^2 u}{4u^2 + \pi^2 l^2} + \frac{4 + 2(-1)^l}{l^2} \qquad (20)$$

Equation 20 implies two well-separated sets of relaxation modes with $l \sim u$ and $l \sim 1$ corresponding to the first and the second terms in the right-hand side; the corresponding relaxation times are $\tau_{fast} \sim \tau_R/u^2 \sim \tau_0/(q^4\alpha^4)$ and $\tau_{slow} \sim \tau_R \sim \tau_0 N^2$. The fast modes with $\tau_{fast} \propto q^{-4}$ were first predicted in ref 26 for a homopolymer system (in the regime $qR_g \gg 1$, block copolymers and homopolymers should show similar relaxation behavior). However, the slow modes with Rouse relaxation time τ_R were overlooked.[26] Physically, the slow modes represent the effect of chain tails, whereas the fast modes are due to relaxation of internal parts of chains. Note that the slow modes are not really negligible as their amplitude, $J_{slow} = \sum_l 2\pi^2 u/(4u^2 + \pi^2 l^2)$, is actually equal to that of the fast modes: $J_{slow} = J_{fast} = \pi^2/2$. Alternatively, in the $u \ll 1$ limit, $J_l \cong 2u/l^2$, and, thus, the main contribution to the intensity I_R arises from the main mode, $l = 1$; higher-order Rouse modes can be neglected within a semiquantitative treatment. The same qualitative situation also holds for the intermediate region, $u \sim 1$ (i.e., for $qR_g \sim 1$).

The generalization for the case of semidilute solutions ($\phi < 1$) in a good solvent is straightforward by carrying through the renormalizations described in section II.1. Thus, the time of the main ($l = 1$) Rouse mode is given by eq 13a, while its intensity (see eq 18) is $I_R = (1/6\pi^2)\phi N_e(\phi) J_1$, where $J_1 = J_1(u)$ is defined in eq 19. In particular for $u \ll 1$ one gets

$$I_R = \frac{1}{6\pi^2}\phi N_e(\phi) q^2 R_g^2 \qquad (13c)$$

in agreement with eq 13b.

II.3. Scattering by Total Concentration and Composition Fluctuations. The composition fluctuations can relax via the two motional mechanisms described in sections II.1 and II.2. Since these can occur simultaneously at different places, the total scattering function is a sum of the reptation and Rouse contributions, i.e.

$$S(q,t) = S_{rept}(q,t) + S_R(q,t) \qquad (21)$$

with $S_{rept}(q,t)$ and $S_R(q,t)$ given by eqs 4 and 18, respectively.

The total concentration fluctuations, on the other hand, relax via the cooperative diffusion mode.[17,19] Similarly to semidilute solutions of linear homopolymers, the diffusive relaxation rate increases with concentration ϕ, whereas its intensity, I_{coop}, decreases with ϕ in clear distinction with eqs 11 and 13. Further, the two intensities I_{coop} and I_{rept} can be quite different. In fact, for $\chi = 0$, the intensity of the main reptation mode for composition fluctuations is $I_0 \sim (n_A^2 - n_B^2)^2 N\phi$ (eq 11 for $qR_g \sim 1$). On the other hand the intensity of the cooperative mode is $I_{coop} \sim (\bar{n}^2 - n_s^2)^2 \phi g$. Here n_A, n_B, and n_s are the refractive indices of pure A and B components and the solvent, respectively, and $\bar{n}$ is the average refractive index of the copolymer. For a high molecular weight diblock with $N \sim 10^4$, the number of links per blob at a typical concentration $\phi \cong 5\%$ can be estimated as $g \propto \phi^{-1/(3v-1)2} \sim 50$. Therefore, the relative intensity of the cooperative mode is very small: $I_{coop}/I_0 \sim g/N \sim 1/200$.

III. Experimental Section

Materials. The synthesis of the very high molecular weight poly(styrene-*b*-isoprene) diblock, SI-1M, was performed at room temperature in evacuated, *n*-BuLi washed, and benzene rinsed glass reactor, provided with constrictions and break-
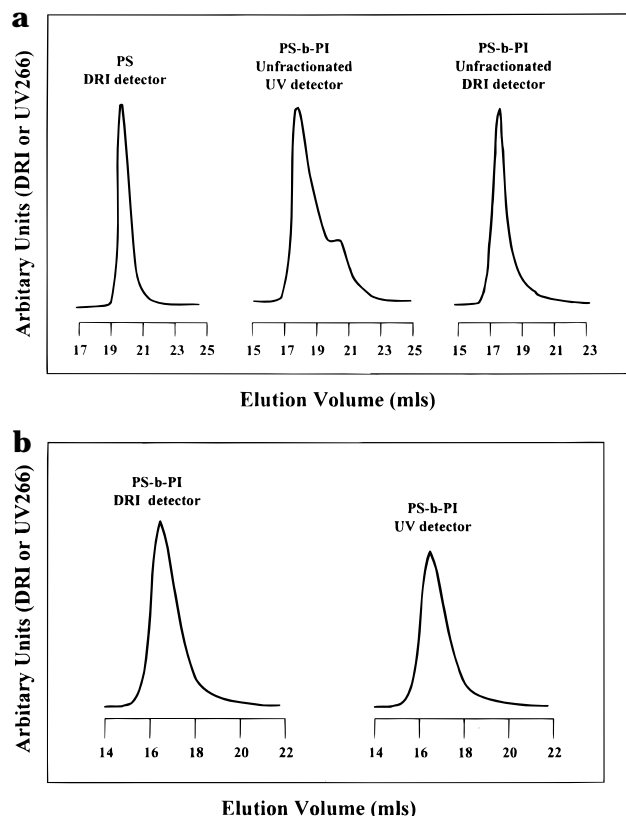
a

b

Figure 1. (a) Size exclusion chromatograms of the polystyrene (PS) precursor and the unfractionated SI-1M diblock copolymer (UV and RI detector). (b) Size exclusion chromatograms (RI and UV detector) of the fractionated SI-1M diblock copolymer.

seals, using *s*-BuLi as initiator. Extra purification procedures for monomers, initiator, and solvents were required due to the very low initiator concentration needed ($\sim 10^{-5}$ mol for 10 g of copolymer), which was carried out in a purged with *n*-BuLi apparatus. Dibutylmagnesium was used for the purification of styrene (Merck) and *n*-BuLi for isoprene (Fluka). Finally, the purified monomers were distilled in purged with *n*-BuLi ampules. The initiator, *s*-butyllithium, was prepared from *s*-butyl chloride and lithium dispersion. Following this procedure, the initiator was diluted in a purged with *n*-BuLi apparatus with calibrated ampules. Initially, the poly(styryllithium) block was prepared and a small aliquot was removed for characterizaton (Figure 1a). The polymerization was completed after the addition of the isoprene monomer and took 2 days.

Fractionation of the final diblock copolymer was performed, in several steps, by adding methanol (nonsolvent) to the copolymer solution (~ 0.1 vol %) in a mixture 1:1 by volume of toluene (solvent for both blocks) and hexane (solvent for PI). The fractionation was monitored by size exclusion chromatography (SEC, THF, 30 °C) with differential refractive index (DRI) and UV detector operating at 266 nm (UV266). The UV detector at 266 nm monitors only the polystyrene part of the copolymer. The SEC traces of the unfractionated copolymer (Figure 1a) revealed some expected termination of the poly(styryllithium) by the minimal yet unavoidable impurities in the added isoprene. The impurities are very influential due to the active centers. The terminated polystyrene precursor was removed by the fractionation, as shown in Figure 1b.

Low-angle laser light scattering (LALLS, THF, 25 °C), laser differential refractometry (THF, 25 °C, d*n*/d*c* = 0.150 mL/g), ^{1}H- NMR (CDCl$_3$, 30 °C), and UV (THF, 269 nm) measurements were performed for molecular and compositional characterization; the characteristics of the diblock and of the polystyrene precursor are shown in Table 1. These results indicate a high degree of molecular and compositional homogeneity. Very high molecular diblocks have been synthesized before,[30] as well, for the investigation of their optical properties.

Table 1. Sample Characteristics

species	$M_w{}^a$	M_w/M_n	PS content	N^e	$f_{PS}{}^f$	$\phi_{ODT}{}^g$
PS block	4.65×10^5	1.05	1.000	5210	1.000	
SI-1M	1.04×10^6	1.10	0.447^b	12477	0.413	between 7.1 and 7.5 wt %
			(0.442^c)			
			(0.444^d)			

^{a} By low angle laser light scattering in THF. ^{b} Calculated from the M_w's of the PS precursor and the diblock. ^{c} By ^{1}H-NMR. ^{d} By UV. ^{e} Based on average segmental volume for both the diblock and the PS block. ^{f} Polystyrene volume fraction. ^{g} Obtained from depolarized dynamic light scattering.

A very low concentration (<0.5% by weight) copolymer solution in HPLC grade toluene solvent is initially prepared and filtered through a 0.22 μm Millipore filter directly into the dust-free light scattering cell (10 mm). During the measurements the cell was closed air-tight to avoid evaporation of toluene. The concentration was checked before and after each measurement by weighing the solution. The concentration is then gradually increased by slow evaporation of small amount of solvent and weighing the resulting solutions. All the concentrations reported here (2.4−7.5 wt %) are well above the overlap concentration $c^* \cong 0.2$ wt %.

Photon Correlation Spectroscopy (PCS). The autocorrelation function of the polarized light scattering intensity, $G_{VV}(q,t) = \langle I_{VV}(q,t)I_{VV}(q,0)\rangle/\langle I_{VV}(q,0)\rangle^2$, with $I_{VV}(q,0)$ the mean light scattering intensity, is measured at different scattering angles, θ, using an ALV spectrophotometer and an ALV-5000 full digital correlator over the time range 10^{-7}–10^3 s. Both the incident beam from an Adlas diode pumped Nd-YAG laser, with wavelength $\lambda = 532$ nm and single mode intensity 160 mW, and the scattering beam were polarized perpendicular (V) to the scattering plane. $q = (4\pi n/\lambda)\sin(\theta/2)$ is the magnitude of the scattering vector, with n the refractive index of the medium. In quasi-elastic light scattering under homodyne conditions, $G_{VV}(q,t)$ is related to the desired relaxation function, $C(q,t)$, by

$$C(q,t) = \{[G_{VV}(q,t) - 1]/f^*\}^{1/2} \qquad (22)$$

where f^* is an experimental factor calculated by means of a standard. The amplitude $a \leq 1$ of the $C(q,t)$ is the fraction of $\langle I_{VV}(q,0)\rangle$ with decay times slower than about 10^{-7} s.

Figure 2 shows the q-dependence of $I_{total} \equiv \langle I_{VV}(q,0)\rangle$, the total light scattering intensity normalized to that of toluene for the SI-1M solutions in toluene as a function of copolymer concentration. The significant q-dependence at higher concentrations is due to the correlation hole maximum[12] in disordered diblocks near q_c; the very high MW of the diblock allowed the investigation of this regime by light scattering, although only the left side of the peak could be measured in the available light scattering q-range. In the inset, a dramatic increase of the scattering intensity for the 7.5 wt % solution as compared to 7.1 wt % is evident, as well as a much sharper q-dependence for the 7.5 wt %, due to the transition to the ordered state; this is verified by depolarized light scattering,[31] to be presented separately.[32] As will become evident below, this increase in the total light scattering intensity is essentially associated with the main internal block copolymer relaxation discussed in section II.1.

IV. Data Analysis

The high quality of the intermediate scattering function $C(q,t)$ over a broad time range (see figures below) facilitates the unambiguous extraction of detailed information with regard to the number of distinct relaxation modes and the shape of the dominant structural relaxation process near q_c (eq 21) in an interacting diblock copolymer system. We perform below an interactive data analysis, in the sense of mutual consideration of experimental and theoretical evidence, proceeding from the classical cumulant to the Laplace inversion technique.
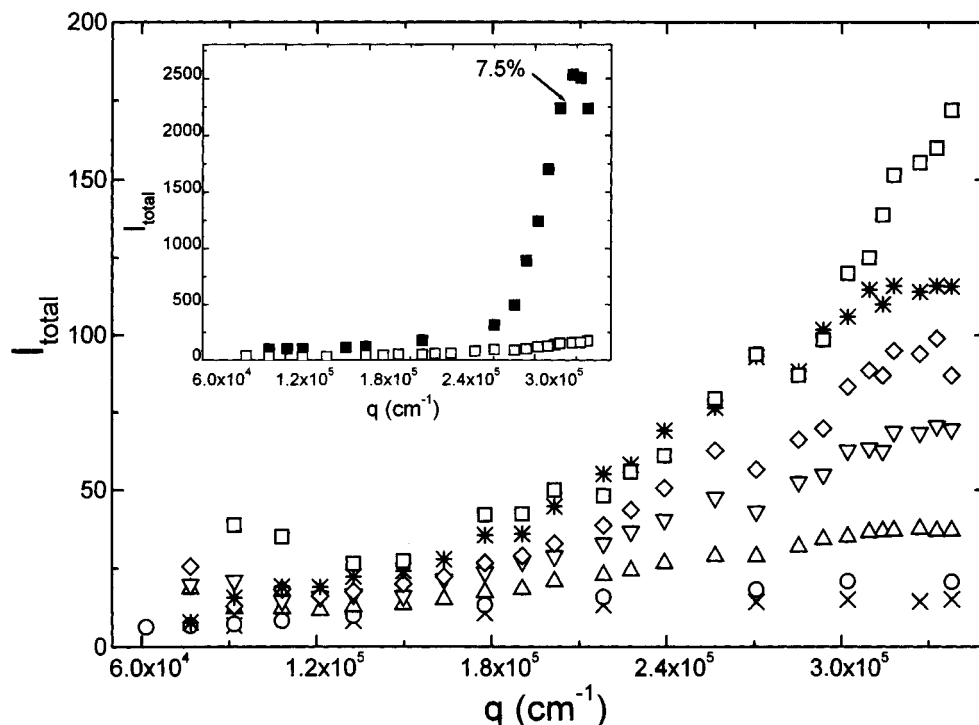
Figure 2. Total polarized static light scattering intensity normalized to that of toluene versus the wavevector for a series of SI-1M solutions in toluene at various concentrations: ($\times$) 2.4; ($\bigcirc$) 3.3; ($\triangle$) 4.8; ($\triangledown$) 5.9; ($\diamondsuit$) 6.2; ($\ast$) 6.5; ($\square$) 7.1; ($\blacksquare$) 7.5 wt %.
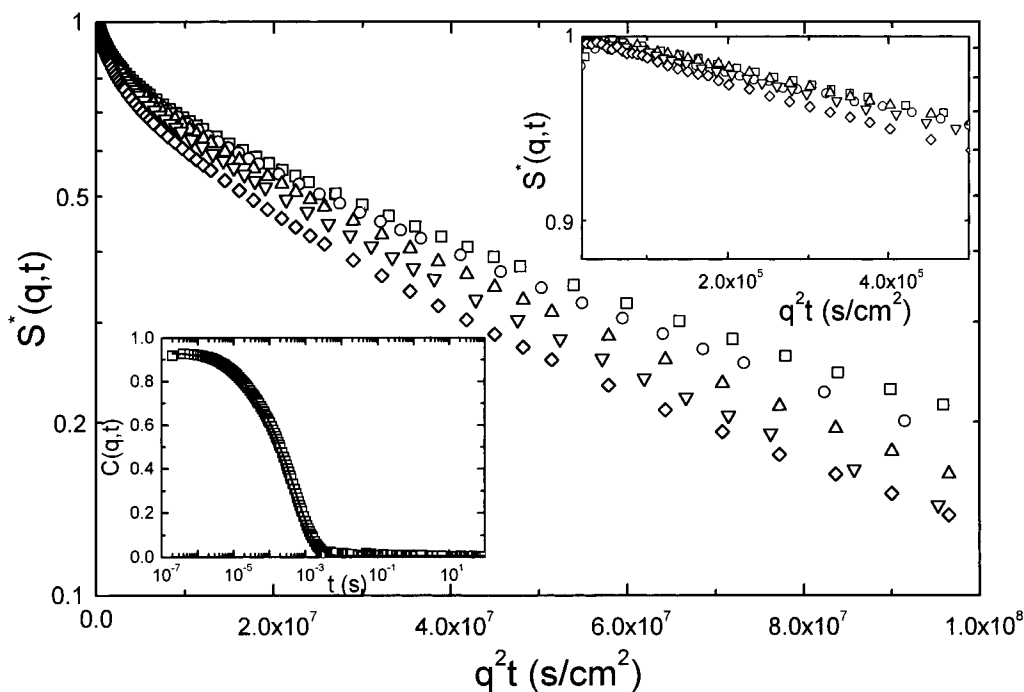

Figure 3. Normalized intermediate scattering function $S^*(q,t)$ for the 2.4 wt % SI-1M/toluene solution at 23 °C for five scattering angles 150° ($\square$), 115° ($\bigcirc$), 90° ($\triangle$), 75° ($\triangledown$), and 60° ($\diamondsuit$) plotted against q^2t. Upper inset: short-time behavior. Lower inset: relaxation function $C(q,t)$ for $q = 0.034$ nm^{-1} ($\theta = 150°$) versus time.

IV.1. Cumulant Technique. In this section, we examine $C(q,t)$ at two extreme concentrations far and near ϕ_{ODT} at 23 °C but much above the overlapping ϕ^*. Figure 3 shows the normalized intermediate scattering function $S^*(q,t) \equiv S(q,t)/S(q) = C(q,t)/a$ versus q^2t for 2.4 wt % solution ($\phi \cong 12\phi^*$), and five different wavevectors between 0.018 and 0.034 nm^{-1} at 23 °C. The attainability of a plateau at short times of the experimental $C(q,t)$, plotted versus time in the lower inset of Figure 3 does not impose a significant error in the normalization procedure. The value of the amplitude a compares well with that obtained from the representation of $C(q,t)$ by a superposition of exponentials (eq 25 below) and/or double stretched exponentials [exp($-(t/\tau)^\beta$), $\beta \leq 1$, eq 24], where applicable. The representation by the cumulant expression

$$\ln C(q,t) = \ln a - Dq^2t + \frac{1}{2!}\mu_2 D^2(q^2t)^2 - \frac{1}{3!}\mu_3 D^3(q^2t)^3 + \ldots \quad (23)$$

results in only a moderate fit quality in the examined ϕ range (discussed also below) and, thus, cannot provide reliable values of a. The lack of superposition of
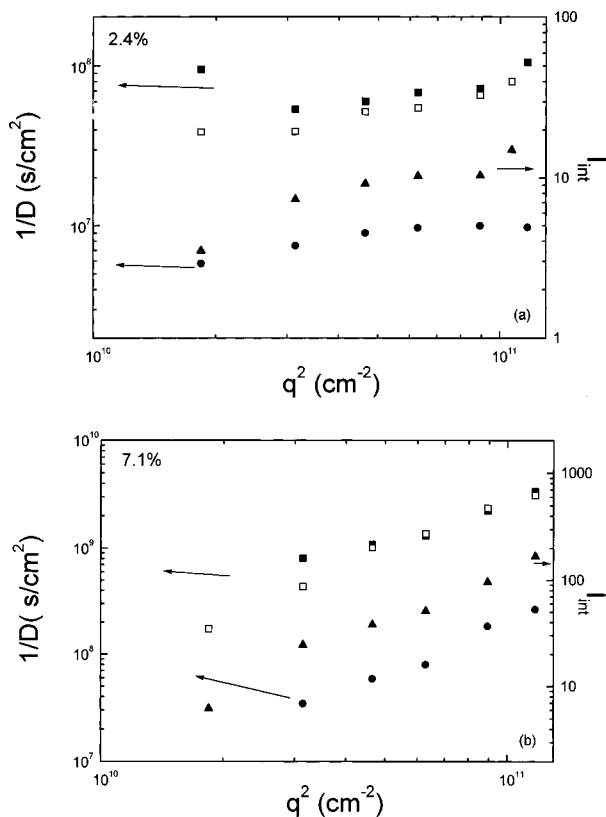
Figure 4. Short- (●) and long-time (■) effective diffusion coefficient for (a) the 2.4 and (b) the 7.1 wt % SI-1M/toluene solutions at 23 °C plotted in reciprocal form versus q^2. For comparison, the inverse of the effective diffusion coefficient $D = \Gamma_{int}/q^2$ (□) and the intensity I_{int} (▲) of the main relaxation process obtained from the ILT of the $C(q,t)$, eq 25, are also shown.

$S^*(q,t)$ vs q^2t in Figure 3 clearly demonstrates nondiffusive (q^2t) behavior and indicates the presence of distinct relaxations in contrast to the single translational diffusion below ϕ^*. Hence, eq 23 cannot adequately describe the strongly nonexponential total $C(q,t)$ over the whole q^2t range.

Similarly to the dynamics of density fluctuations in hard sphere colloids,[33] one may describe the decay of $C(q,t)$ separately at short (upper inset of Figure 3) and long times (Figure 3) by single exponentials; such fits define an initial short-time diffusion coefficient, $D_{in}(q)$, and a long-time diffusivity, $D_L(q)$, both shown in Figure 4a. The presence of at least two relaxation processes is conceivable since total concentration, $\phi = \phi_A + \phi_B$, and composition, $\eta = \phi_A - \phi_B$, fluctuations relax by cooperative and structural relaxation, respectively (see section II.3). While the relaxation rate of the former is purely diffusive ($\Gamma_c = D_c q^2$), the characteristic relaxation rate of the latter deviates from the q^2-dependence, i.e., $D(q) = \Gamma(q)/q^2$ depends on q. The q-dependence of D_L-(q) plotted in reciprocal form for comparison with I_{int}-(q), the intensity of the main mode obtained from the inverse Laplace analysis below, supports the relation $D_L(q) \sim [I_{int}(q)]^{-1}$. However, the initial $D_{in}(q)[= \{1 - a(q)\}D_c + a(q)D(q)]$ decreases also with q, because of the apparent reduction of the relative amplitude of the cooperative mode, $\{1 - a(q)\}$.

The similarity between the amplitudes of the two processes and the closeness of the rates at this concentration hinders a detailed shape analysis. However, the simplest double exponential fit to the experimental $C(q,t)$ at $q = 0.018$ nm^{-1} ($\theta = 60°$) and $q = 0.034$ nm^{-1} ($\theta = 150°$) yields clearly systematic deviations. Since

concentration fluctuations decay exponentially with a faster rate Γ_c, we replace the second exponential by a stretched one for the dynamics of the composition fluctuations. In fact, this function can represent well these two typical correlations with $\tau_c = 62$ μs, $\tau = 1.1$ ms, and $\beta = 0.63$ for $\theta = 60°$ and $\tau_c = 17$ μs, $\tau = 0.49$ ms, and $\beta = 0.72$ for $\theta = 150°$; $\Gamma_c = 1/\tau_c$ scales expectedly with q^2. An unexpected finding is the apparent nonexponential shape of the structural relaxation revealed also from the cumulant analysis (eq 23) of the long-time decay of $C(q,t)$ ($q^2t > 10^7$ s/cm^2) where μ_2 amounts to 0.25 and 0.12, respectively, for $\theta = 60°$ and 150°. Due to the reverse concentration dependence of the cooperative and the structural relaxation processes, the resolution of these modes should increase at higher concentrations.

Figure 5 shows the experimental $S^*(q,t)$ for the 7.1 wt % solution ($\phi \cong 35\phi^*$) near ϕ_{ODT} at four different wavevectors. While the nondiffusive decay is obviously retained, the nonexponentiality (deviation from the slope -1) of $C(q,t)$ at long times and for the highest wavevector near q_c (Figure 2) is significantly reduced. At this wavevector, the structural relaxation dominates and $C(q,t)$ can provide information on the detailed shape of the temporal decay for the most probable composition fluctuations with wavevector $q \sim q_c$. The single exponential decay at long times (solid line in Figure 5) covers more than 1 decade in time necessary to relax it; deviation at short times suggests the presence of additional fast process(es). This becomes evident from the failure of eq 23 to describe the full $C(q,t)$ and the applicability of the function

$$C(q,t) = a_f(q) \exp[-(\Gamma_f t)^{\beta_f}] + a(q) \exp[-\Gamma_L t] \qquad (24)$$

to represent the experimental $C(q,t)$. The distribution parameter $\beta_f = 0.4$ for the fast process(es) is significantly less than 1 implying a broad distribution of relaxation rates Γ_f. Since long wavelength total polymer concentration fluctuations decay exponentially with $\Gamma_c = D_c q^2$, this low value of β_f indicates the presence of an additional fast process in $C(q,t)$ at short times. To elucidate the short time dynamics, we examine the shape of $C(q,t)$ after subtraction of the slower exponential decay (second term in eq 24). As shown in the upper inset of Figure 5 for two wavevectors, this strongly nonexponential fast decay cannot be well represented by the cumulant expression of eq 23. Therefore, the analysis is not consistent with a single broad process at early times but it provides evidence for an extra decay. Indeed, a bimodal function similar to eq 24 was found to provide much better fit to this fast part of the correlation function (in the inset of Figure 5) with exponent 0.9. Taking the exponentiality of the fastest cooperative diffusion process for granted, the analysis of the early and intermediate time decay reveals the diffusive nature of the cooperative process as well as an extra process (faster than the slower process in Figure 5), which bears the characteristics of the predicted Rouse mode (section II.2); its intensity increases with q, whereas its relaxation rate is q-independent (see eq 13). Note the diffusive (q^2t) scaling only for the initial decay of $S^*(q,t)$ in the inset of Figure 5. As a matter of fact, a sum of three exponentials can well represent the full $C(q,t)$.

On the basis of these findings, it is evident that three relaxation processes control the intermediate scattering function of the SI-1M near ϕ_{ODT} at $q \sim q_c$. The dominant contribution ($\cong 92\%$ of the total amplitude) arises from
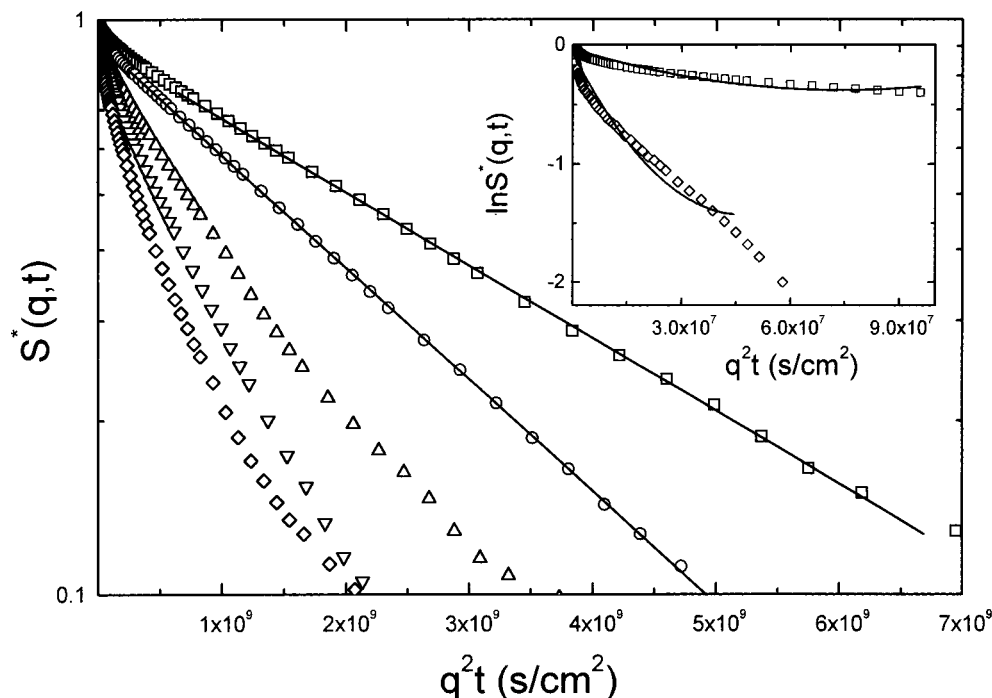
Figure 5. Normalized intermediate scattering function $S^*(q,t)$ for the 7.1 wt % SI-1M/toluene solution at 23 °C for five scattering angles 150° (□), 115° (○), 90° (△), 75° (▽), and 60° (◇) plotted against q^2t; corresponding q values were 0.018–0.034 nm^{-1}. The solid lines represent a single exponential decay. Inset: short-time behavior for $q = 0.018$ nm^{-1} ($\theta = 60°$) and 0.034 nm^{-1} ($\theta = 150°$) versus q^2t where the lines are the best fits with eq 23, which cannot represent the data.

the structural relaxation due to rearrangements of the two blocks and exhibits an exponential shape (eq 4), in agreement with the predicted small nonexponentiality factor, $[\Omega(q)T(q) - 1]$, near ODT. Its effective diffusion coefficient, $D_L(q) = \Gamma_L(q)/q^2$, describing the decay of composition fluctuations with wavevector q is shown in Figure 4b along with the short time D_{in}, and the intensity of the main mode $I_{int}(q)$. The observed q-dependence is clearly much stronger near than far (Figure 4a) from ϕ_{ODT}. The strong q-dependence of D_L-(q,t) resembles that of $I_{int}(q)$ reflecting the effects of the thermodynamic interactions. Near ϕ_{ODT}, $D_{in} \cong [1 - a(q)]D_c$ shows also a strong q-dependence compared to the 2.4 wt %, which is again due to the stronger q-dependence of $a(q)$. The strong evidence for the presence of three relaxation processes in the experimental $C(q,t)$ in the concentration regime 3.3 to 7.1 wt % supports the delicate Laplace inversion for a quantitative description of the full dynamic structure factor.

IV.2. Laplace Inversion. Figure 6a shows the net polarized intensity autocorrelation functions, $C(q,t)$, for the 4.7 wt % SI-1M solution at 23 °C and various scattering angles. The experimental correlation functions are analyzed by performing the inverse Laplace transform (ILT) of $C(q,t)$, without assumption of the shape of the distribution function $L(\ln \tau)$ but assuming a superposition of exponentials:

$$C(q,t) = \int_{-\infty}^{\infty} L(\ln \tau) \exp[-t/\tau] \, d(\ln \tau) \qquad (25)$$

This determines a continuous spectrum of relaxation times $L(\ln \tau)$; the average times obtained from the peaks of $L(\ln \tau)$ are used to determine the characteristic relaxation times, whereas the integral under the peaks of $L(\ln \tau)$ gives the dynamic intensity associated to the specific relaxation. For comparison, the distributions $L(\ln \tau)$ multiplied by I_{total}, the total polarized intensity normalized to that of toluene, are shown in the inset of Figure 6a for various angles. Figure 6b shows $C(q,t)$ for the 7.1 wt % SI-1M solution at 23 °C and various

scattering angles, whereas the inset shows the wavevector dependencies of the relaxation times and the respective intensities of the processes identified by the ILT procedure as in the inset of Figure 6a. The relaxation rate and intensity of the main (slower) process are also shown in Figure 4b.

Three relaxation processes are observed to contribute to the experimental correlation functions, in agreement with their cumulant analysis above (section IV.1). The characteristics of the fast mode are a q-independent amplitude (inset of Figure 6b) which decreases with increasing concentration (it is barely seen for 4.7 wt % in Figure 6a, whereas it is much more pronounced at lower concentrations[16]) and a relaxation rate that shows a q^2-dependence (Figure 6b) with a diffusion coefficient which becomes faster when concentration increases (not shown). According to the discussion in the theoretical section II.3, this process is the well-known cooperative diffusion mode of the copolymer molecules[6] above the overlap concentration, that corresponds to the relaxation of the total polymer concentration and is similar to the mode observed in homopolymer solutions; this is verified by PCS measurements on solutions of a 1.1×10^6 MW polystyrene in toluene.

The amplitude of the main slower process increases significantly as concentration increases, whereas its dynamics becomes slower. Its intensity exhibits a noteworthy wavevector dependence, i.e., it increases significantly at higher wavevectors; note that, in most of the situations investigated with dynamic light scattering, the intensities are either independent of q (e.g., for the cooperative diffusion discussed above or for the polydispersity diffusive relaxation[4,6,10] in diblock copolymers or the interdiffusion in polymer blends[1d,e]) or they increase at low wavevectors when large scatterers are involved. The present behavior reflects the q-dependence of the total polarized light scattering shown in Figure 2; i.e., it is related to the correlation hole peak in disordered diblock copolymers. At the same time, the relaxation rate of the slower process exhibits a weak q
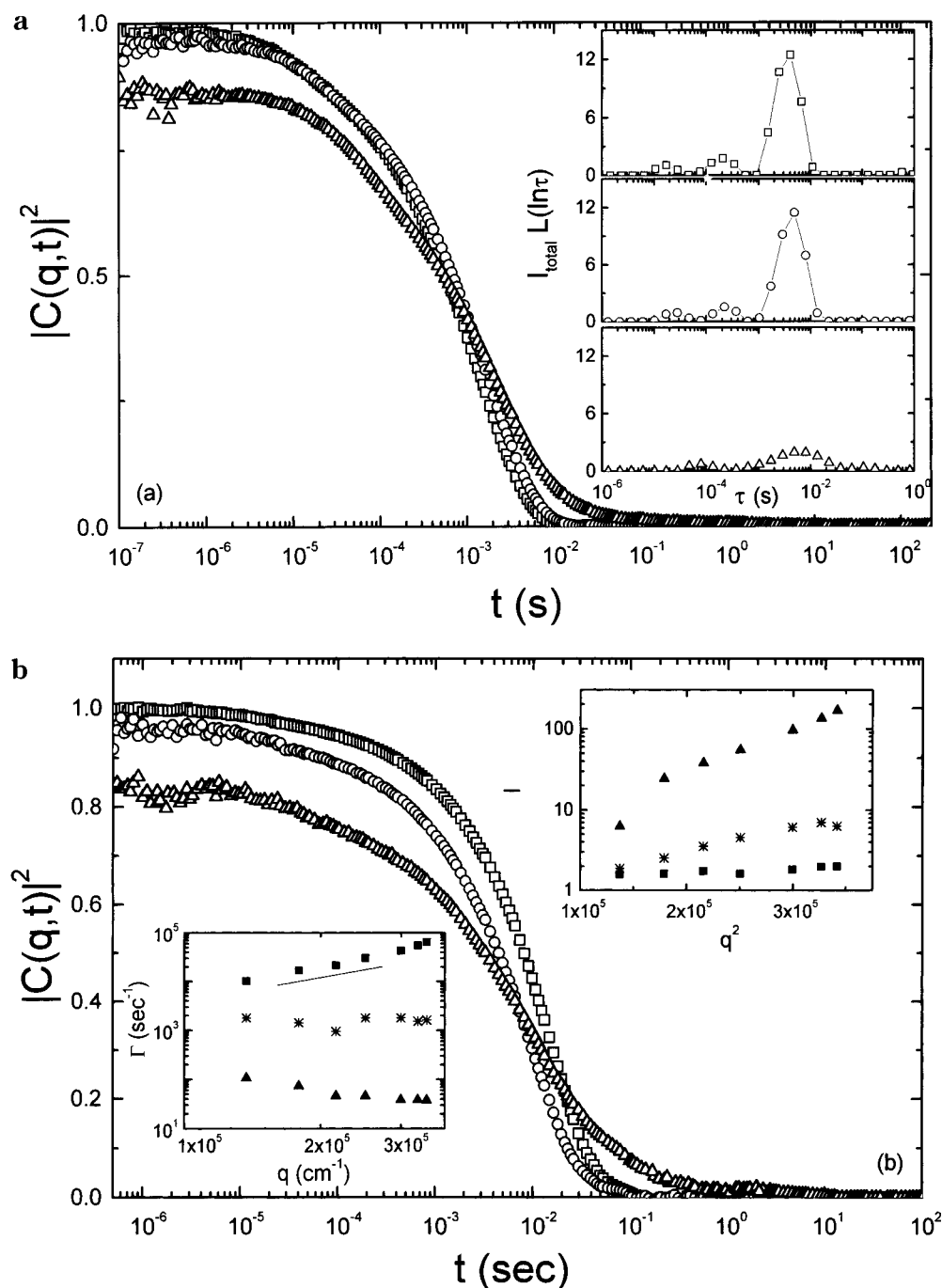
Figure 6. (a) Correlation function $C(q,t)$ for a 4.7 wt % disordered SI-1M/toluene solution at 23 °C for three scattering angles 135° (□), 90° (○), and 45° (△). The distribution of relaxation times obtained from the ILT of the experimental correlation functions multiplied by the total polarized intensities normalized to the intensity of toluene are shown in the inset. (b) Correlation function $C(q,t)$ for a 7.1 wt % disordered SI-1M/toluene solution at 23 °C for three scattering angles 150° (□), 90° (○), and 45° (△). The wavevector dependence of the normalized polarized intensities (upper inset) and of the relaxation rates (lower inset) for the three relaxation processes obtained from the inverse Laplace transform analysis: (■) cooperative diffusion, (▲) internal block copolymer mode, and (*) newly discovered process attributed to Rouse-like motions of the blocks between entanglements inside their tubes. The solid line in the lower inset indicates slope 2.

dependence for the 4.7 wt %, whereas it shows a slight slowing down as the wavevector increases for the 7.1 wt %. This variation with q is in accordance with the q-dependence of the effective $D_L(q)$, eq 24, of Figure 4b. As will be discussed below, this slowing down is due to thermodynamics, i.e., due to the solution approaching the ordered state. An even stronger slowing down is observed for the 7.5 wt % solution, which is ordered but very close the ODT. This is the main internal copolymer mode discussed earlier.

The intermediate mode is a new process that was observed for the first time in the present SI-1M/toluene system;[16] it appears in the correlation function only

above about 3 wt % and, overall, its characteristics show a weaker wavevector dependence than the internal mode. Moreover, its intensity is about one-tenth that of the internal mode and its relaxation rate is about 1 order of magnitude faster. In our earlier paper,[16] this process was attributed to Rouse-like chain conformational relaxation within the reptation tube based on a good agreement of the experimental findings with semiquantitative theoretical predictions (eq 13). Below, we will show that this assignment is further supported by the agreement with the quantitative theoretical approach presented in section II.2 above.
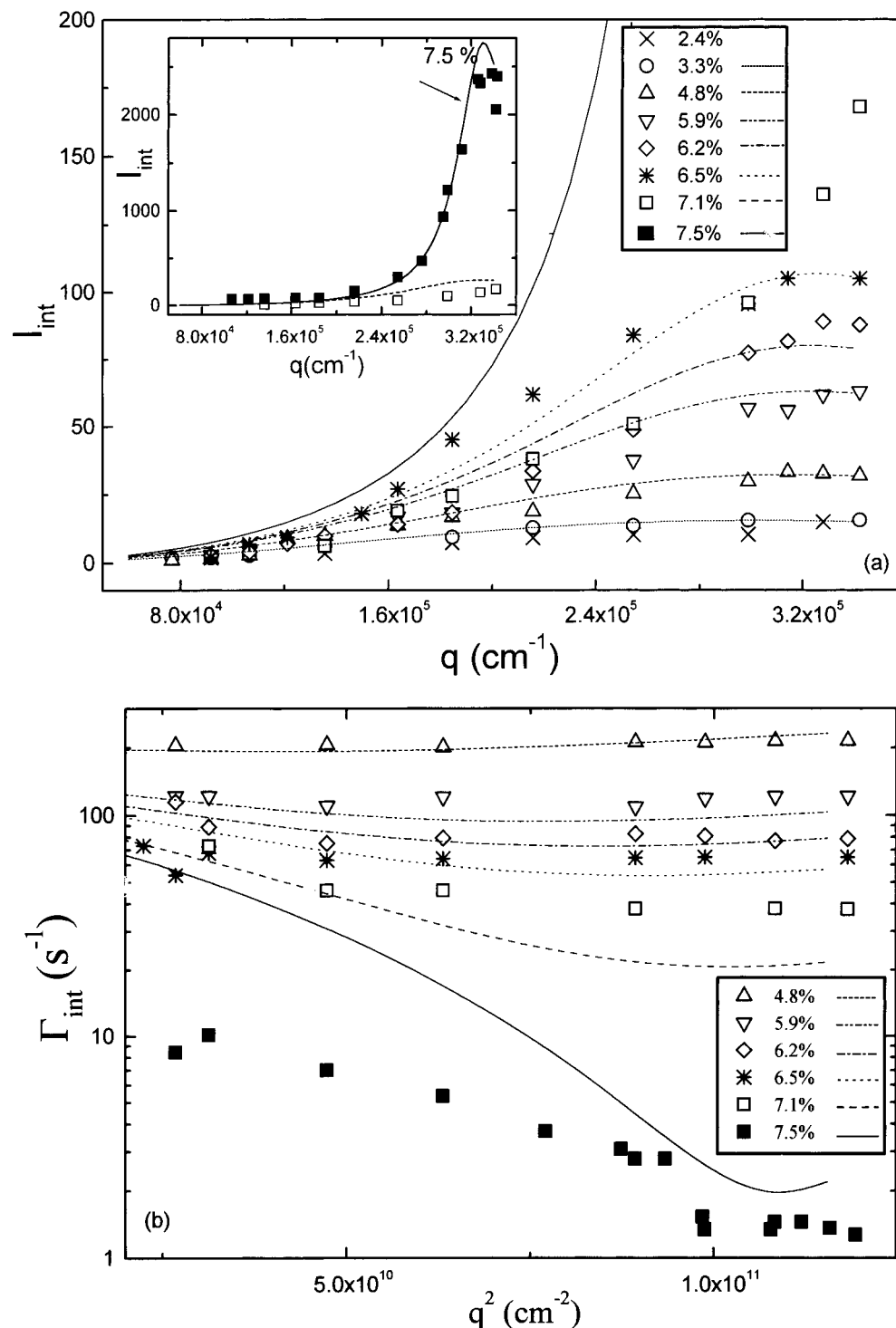
Figure 7. Wavevector dependence of (a) the normalized polarized intensities and (b) the relaxation rates for the internal process for the SI-1M/toluene solutions for various concentrations. Symbols denote different concentrations shown in the legend. Lines denote the predictions according to theory presented in section II.1.

V. Comparison with the Theoretical $S(q,t)$

The main mode in the experimental $S(q,t)$ is always the slow process, which is the internal block copolymer relaxation process. This relaxation mode is identified with the main reptation mode discussed in section II.1. The intensity $I_{int} = I_{k=0}$ and the relaxation rate $\Gamma_{int} = \Gamma_{k=0}$ of this mode are defined in eqs 4, 5, and 11 ($k = 0$ corresponds to the lowest rate, i.e., the lowest Γ_k).

In order to compare the experimental data with the theoretical predictions, one needs to determine the concentration dependence of the molecular weight between entanglements, N_e. Since there is no formal theory accounting for either the effective N_e for a block

copolymer or the $N_e(\phi)$ dependence in the whole concentration range, $N_e(\phi)$ for the diblock copolymer is estimated using the data for pure polymers[34] and a mixing rule proposed for the plateau modulus of a homogeneous polymer blend[35] (already applied before[36] for block copolymers). The results in the concentration range 3–7.5% can be empirically represented by $N_e(\phi) \cong 94/\phi$. Thus, the number of entanglements per chain, $n_e = N/N_e(\phi)$, varies in the range $n_e = 4$–10.

Figure 7 shows the comparison between the experimental results for the intensity (Figure 7a) and the relaxation rate (Figure 7b) of the internal copolymer mode and the theoretical predictions for I_0 and Γ_0 (for k

= 0) for different concentrations as a function of the scattering wavevector. As also indicated in Figure 6, the q-dependence of the intensity mirrors that of the total scattering intensity signifying that the dependence in Figure 2 is essentially due to this process. When the solution attains the ordered state (7.5 wt %), there is again a dramatic increase of the intensity associated with this particular process. The relaxation rate of the mode displays subtle changes with the wavevector (see also Figure 4) for all the concentrations up to 6.5 wt %; it shows a weak slowing down with increasing wavevector for the 7.1 wt % solution (shown in Figures 4 and 6b and discussed before), whereas a dramatic q-dependence is observed for the 7.5 wt % solution (the relaxation rate decreases by an order of magnitude with increasing q) together with a significant slowing down of the rate compared to the 7.1 wt % solution. These findings are due to the thermodynamic effects, which control the rate of the main internal diblock chain relaxation where the significant increase (by a factor of 10) in the static structure factor is accompanied by a significant (by 1 order of magnitude) slowing down of the relaxation rate.

The predictions for I_0 and Γ_0 for different concentrations are shown as lines compared with the data in parts a and b of Figure 7, respectively, with the thermodynamic incompatibility (χN) and the size of the diblock (Nb^2) treated as adjustable parameters. Besides, an independent of concentration multiplication factor for the intensities was used, since the intensity data were not converted to absolute structure factors (the changing number of scatterers by increasing concentration is explicitly accounted in the theory, eq 2). The best simultaneous fit for both the intensities and the relaxation rates as a function of concentration and wavevector is obtained for $\chi N \cong 639$, $Nb^2 = 1.14 \times 10^{-10}$ cm^2. With $N \cong 12\,477$, these values correspond to $\chi \cong 0.051$, close to literature values,[31] and $b \cong 9.6$ Å; the obtained b is larger than the usual value $\cong 7$ Å by a factor $\gamma = 1.37$, probably due to additional stretching of diblock copolymer chains in the transition region,[37] which leads to a larger apparent statistical segment length. The factor $\gamma = 1.37$ is in good agreement with a computer simulation result,[38] $\gamma = 1.35$, obtained in the vicinity of the critical point, as well as recent experiments.[39] Besides, the obtained values of χN and Nb^2 imply that the critical concentration $\phi_C \cong 7.5\%$ (see eq 8), and the critical wavevector $q_c = 3.3 \times 10^5$ cm^{-1} ($\cong 1.95/R_g(\phi)$ and eq 6). The consideration of only a single ($k = 0$, eq 4) mode is justified at least for the higher concentrations ($\phi \le \phi_{ODT}$) by the almost exponential shape of the experimental relaxation.

The theory presented in section II.1 adequately describes the concentration and the wavevector dependencies of both the intensity and the relaxation rate of the internal copolymer mode. The most noticeable differences are obtained for the 7.5% solution in the low wavevector regime: Here the observed intensity is about 5 times higher and the relaxation rate is 5 times slower than that predicted. This discrepancy might be explained by extra light scattering at low wavevectors because of the large-scale domain structure in the already ordered[6] 7.5% solution and the theory being applicable only in the disordered state. However, the systematic dependence of the rate on the scattering intensity (also shown in Figure 4) is a consequence of the relation of the collective dynamics to the thermo-
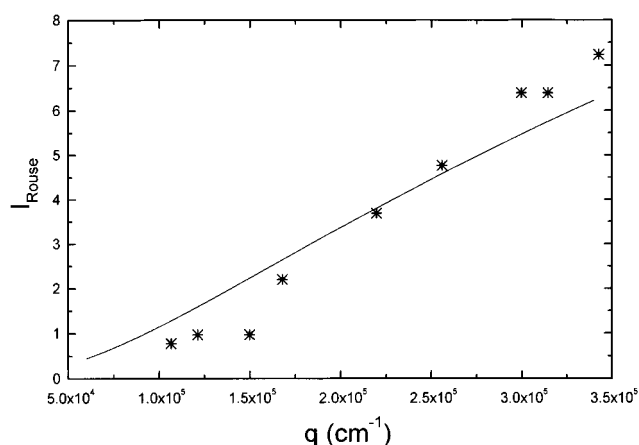

Figure 8. Wavevector dependence of the normalized polarized intensities of the new process (Rouse) for the 6.5 wt % SI-1M/toluene solution. The line shows the predictions according to theory presented in section II.2 and using the parameters obtained by fitting the data for the internal mode (Figure 7).

dynamic interactions,[3,40,41]

$$\Gamma_{int}(q) = q^2 \Lambda g_1(q)/I_{int}(q) \qquad (26)$$

where $g_1(q)$ is the Debye function and Λ the Onsager coefficient; Λ is found nearly q-independent for low concentrations ($\Lambda \sim q^0$), in agreement with the theory, whereas it shows an apparent $\Lambda \sim q^1$ dependence for the 7.5% ordered solution.

Next, attention is focused on the intermediate mode of Figures 5 and 6; the observed new mode is identified with the main ($l = 1$) Rouse mode considered in the theoretical section II.2. This mode is observed only above about 3 wt %, where the solution is entangled ($n_e = N/N_e(\phi) \cong 4$ at 3%). As shown in the insets of Figure 6 and as presented in the earlier paper,[16] the wavevector dependence of this process is similar to that of the internal mode at low concentrations, but both its relaxation rate and its intensity show weaker concentration and wavevector dependencies near the ODT. Figure 8 shows the wavevector dependence of the intensity of this process, I_{Rouse}, for the disordered 6.5 wt % solution together with the predicted wavevector dependence of the intensity of the first Rouse mode I_R (eqs 18 and 19 for $l = 1$) calculated using the same values for the parameters obtained by the fit of the data for the internal mode (Figure 7). It is evident that the theory and the data are in good agreement with respect to the wavevector dependence of the intensity. As for the concentration dependence, eq 13c implies that I_R nearly does not depend on concentration ϕ (a weak ϕ dependence via the parameter $u \propto R_g^2$ can be neglected), whereas the observed intensity is weakly increasing with concentration up to 7.1 wt % and more strongly for the 7.5 wt % solution. The relaxation rate of the Rouse mode, $\Gamma_R = 1/\tau_R$, defined in eq 13a, is independent of the wavevector in apparent agreement with the experimental data. However, the predicted concentration dependence, $\Gamma_R \propto \phi^{(2-3\nu)/(3\nu-1)} \cong \phi^{0.31}$, is much weaker than the observed dependence.[16] The deviations between the theory and the data might be related with the fact that the chains are not really well entangled in the relevant region ($n_e = 4-9$); hence extra effects on the top of the tube model might be expected, as well as the possible concentration dependence of the effective friction coefficient.

The quantitative theory predicts that at low wavevectors the ratios I_0/I_R (eqs 11 and 13c) and Γ_R/Γ_0 (eqs 11
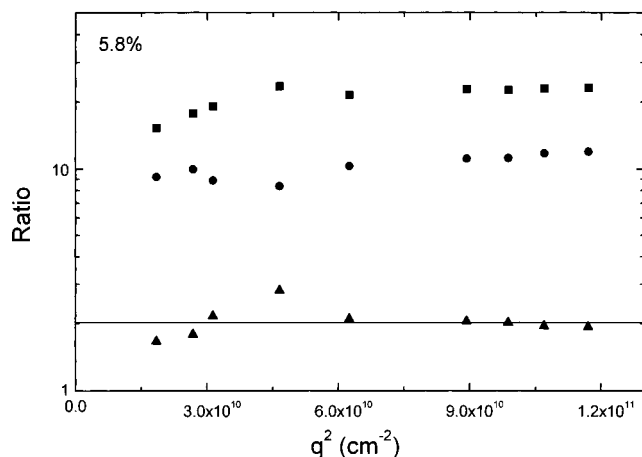
Figure 9. Wavevector dependence of the ratios $\Gamma_{\text{Rouse}}/\Gamma_{\text{int}}$ (■), $I_{\text{int}}/I_{\text{Rouse}}$ (●), and $\{(\Gamma_{\text{Rouse}}/\Gamma_{\text{int}})/(I_{\text{int}}/I_{\text{Rouse}})\}$ (▲) for the 5.8 wt % SI-1M/toluene solution.

and 13a) are nearly constant independent of the wavevector; actually for low qR_g values: $I_0/I_R \cong (24\pi^2)[N/N_e(\phi)]$ and $\Gamma_R/\Gamma_0 \cong [3N/N_e(\phi)]$. Thus, $I_0/I_R \cong 14$ and 21 for the 4.4% and 6.5% solutions, respectively; these values might be compared with the observed ratios at $q^2/q_c^2 \cong 0.4$ of $I_{\text{int}}/I_{\text{Rouse}} \cong 10$ and 16. Moreover, the predicted ratio $\Gamma_R/\Gamma_0 \cong 18$ and 26 to be compared with the experimental $\Gamma_{\text{Rouse}}/\Gamma_{\text{int}} \cong 22$ and 20 for 4.4% and 6.5%, respectively. The agreement between the predictions and the data seems reasonable, taking into account that $n_e = N/N_e(\phi)$ is not very large and the values for $N_e(\phi)$ are quite uncertain. The effects of even higher n_e's are currently investigated using even higher molecular weight diblocks in solution.[42] At the same time, the theory at low wavevectors predicts that the product $\{-(\Gamma_R/\Gamma_0)/(I_0/I_R)\} \cong 3\pi^2/24 = 1.23$, independent of the wavevector and of concentration. This is in agreement with the experimental data (for example for the 5.8 wt % solution shown in Figure 9); the experimental q-independent value for this product for this and for all the other concentrations in the disordered state is about 2 (the q-independent value for the 7.5 wt % solution is about 4).

Therefore, the use of the very high molecular weight diblock copolymer with the inherent contrast between the two blocks not only allowed the investigation of the thermodynamic effects on the internal relaxation process but it also allowed the observation of the Rouse mode predicted in section II.2. Rouse-like fluctuations were only observed using neutron spin echo for homopolymer systems at high wavevectors.[43]

VI. Concluding Remarks

Photon correlation spectroscopy was used to investigate the relaxation of composition fluctuations in disordered diblock copolymer systems near the most dangerous wavevector, q_c. The synthesis of a very high molecular weight diblock copolymer and utilizing semidilute solutions in a common good solvent allowed the detailed investigation of the dynamic structure factor $S(q,t)$ in this wavevector regime near the maximum of the static structure factor. It was found that the relaxation of composition fluctuations in entangled block copolymer solutions proceeds with two different mechanisms associated with reptation motions and Rouse-like motions of chains inside their tubes. The theory adequately describes the combined wavevector and concentration dependencies of the relaxation times and the intensities of the main internal copolymer relaxation

with the effect of the proximity to the disorder-to-order transition (ODT) being evident both in the static light scattering intensity and in the relaxational dynamics by increasing the copolymer concentration to approach the ODT. The second faster process, which is observed in the entangled regime, is predicted by the proposed theory which attributes the mode to another relaxation mechanism due to Rouse-like motions related to curvilinear chain fluctuations inside their tubes. The theory also accounts for the wavevector dependence of the intensity and relaxation rate of this process as well as for the ratio of the intensities and rates of the two processes. However, the observed concentration dependencies of the characteristics of this Rouse mode are stronger than those implied by the theory.

Finally, the polydispersity mode,[4,6,9,10] controlled by the self-diffusivity of the diblock chains, was not observed for this high molecular weight SI-1M/toluene system, because the intensity of the internal process dominates the scattering in this wavevector regime near q_c. The self-diffusivity of the diblock in solution was independently measured by pulsed-field gradient NMR;[44] no process is observed by PCS with behavior corresponding to that of the self-diffusion mode.

Appendix

We present here a rather detailed analysis of the dynamic structure factor for entangled block copolymer melts following the developments in ref 2. The static scattering function, $S(q) = S(q,0)$, for a diblock copolymer melt was calculated using a mean-field approach in the seminal Leibler's paper.[12a] The dynamic structure factor of the system (in the regime of entanglements) was calculated using a mean-field approach and the reptation model[19] as follows:

The average linear response, $\langle \eta \rangle$, of a system to an external perturbation field, U^{ext}, is generally related to the susceptibility of the system, κ, as

$$\langle \eta_q(t) \rangle = -\frac{1}{T}\int \kappa(q,\tau) U_q^{\text{ext}}(t-\tau)\, d\tau \qquad \text{(A.1)}$$

where $U_q^{\text{ext}}(t)$ is the Fourier image of the function $U^{\text{ext}}(r,t) = U_A^{\text{ext}}(r,t) - U_B^{\text{ext}}(r,t)$, with U_A^{ext}, U_B^{ext} being the potentials of the external fields acting on A and B monomers, respectively (T is in units of thermal energy); for a system obeying classical statistics

$$\kappa(q,t) = -\frac{\partial S(q,t)}{\partial t} H(t) \qquad \text{(A.2)}$$

where $H(t)$ is the Heaviside function. To account for the effect of monomer–monomer interactions, the dynamic RPA is employed, which relates the susceptibility κ_0 of the system with no interactions (ideal system) to the susceptibility κ of the interacting system. The arguments are quite simple in the symmetric case. For the ideal system, one can rewrite eq A.1 using the Laplace transformation and assuming that $U^{\text{ext}}(t) = 0$ for $t < 0$ as

$$\eta(q,p) = -\kappa_0(q,p) U^{\text{ext}}(q,p)/T \qquad \text{(A.3)}$$

where $\eta(q,p) = \int_0^\infty \langle \eta_q(t) \rangle e^{-pt}\, dt$, and $\kappa_0(q,p) = \int_0^\infty \kappa_0(q,t) e^{-pt}\, dt$. However, the total field, U, conjugated to the order parameter η is the sum of the external and the molecular contributions, i.e., $U = U^{\text{ext}} + U^{\text{mol}}$, where $U^{\text{mol}} = U_A^{\text{mol}} - U_B^{\text{mol}}$. Equation A.3 is still valid for the

system with interactions provided that U^{ext} is substituted by the total field:

$$\eta(q,p) = -\kappa_0(q,p)[U^{ext}(q,p) + U^{mol}(q,t)]/T \quad (A.4)$$

Note that the excluded volume interactions do not distinguish between A and B links since it is assumed that they are geometrically similar (are characterized by the same volume v) and, hence, these interactions do not contribute to the difference $U_A^{mol} - U_B^{mol}$. However, the incompatibility between A and B links, characterized by the χ parameter, does result in a contribution to U^{mol}. The corresponding free energy term is $F_{int} = \chi T \int \phi_A \phi_B d^3 r/v$; hence, the corresponding contributions to the molecular fields are $U_A^{mol} = v \delta F_{int}/\delta \phi_A = \chi T \phi_B$ and $U_B^{mol} = v \delta F_{int}/\delta \phi_B = \chi T \phi_A$, so that $U^{mol} = -2\chi T \eta$. Therefore, $\eta = -\kappa_0(U^{ext}/T)/(1 - 2\chi\kappa_0) \equiv -\kappa U^{ext}/T$, and the general relation between κ and κ_0 is

$$\frac{1}{\kappa(q,p)} = \frac{1}{\kappa_0(q,p)} - 2\chi \quad (A.5)$$

Equations A.2 and A.5 may be utilized to calculate $S(q,t)$ for an interacting system provided that $\kappa_0(q,p)$ is known; its derivation for the ideal system requires a motional mechanism for the entangled polymer chains. In the reptation model,[19] it is assumed that entanglements of a given chain with the surrounding chains create an effective tube; the confined chain is, thus, considered as a super chain of N/N_e topological blobs with N_e monomers per blob. The tube diameter, d_e, is equal to the size of a topological blob, $d_e \cong b N_e^{1/2}$, and the tube length is $L_t \cong d_e N/N_e$. The principle chain motion on scales larger than d_e is a reptation along the tube axis, s, which is, in fact, an one-dimensional curvilinear diffusion with diffusion constant $D_t = T/(N\zeta_0)$, where ζ_0 is the friction constant per link. Neglecting the tube-length fluctuations (their effect is considered in section II.2), the curvilinear distance between any two links, n and n', is constant: $s(n) - s(n') = L_t(n - n')/N$. During a short time Δt, the nth link diffuses along the tube over a distance Δs, with $\langle(\Delta s)^2\rangle = 2D_t\Delta t$ to the point, where the $(n + \Delta n)$th link was originally located, with $\Delta n = (N/L_t)\Delta s$ and, thus, $\langle(\Delta n)^2\rangle = 2D^*\Delta t$, where $D^* = (N/L_t)^2 D_t$. Therefore the distribution function, $f_n(\mathbf{r},t)$, for the position $\mathbf{r}$ of the nth link obeys the diffusion equation

$$\frac{\partial f_n(\mathbf{r},t)}{\partial t} = D^* \frac{\partial^2 f_n(\mathbf{r},t)}{\partial n^2} \quad (A.6)$$

Note that eq A.6 is valid for a system with no excluded-volume interactions, i.e., when there is no molecular (or external) field which could affect the reptation process. In the reptation model, the very end parts of the chains relax extremely fast, and, hence, $f_n(\mathbf{r},t)$ at the end must obey the Edwards equilibrium equation[19] $\partial f_n(\mathbf{r},t)/\partial t = \pm\alpha^2\nabla^2 f_n$ for $n = 0$, N with $\alpha = b/\sqrt{6}$.

Next, one proceeds with the calculation of the structure factor $S_0(q,t)$ of the system with no interactions between monomers (apart from the topological ones) in order to calculate $S(q,t)$ for the original interacting system ($\chi \neq 0$) using eqs A.2 and A.7. Equation 1 in the main text can be rewritten as

$$S_0(q,t) =$$
$$\frac{\phi_0}{4N}\int dn\, dm\, \langle\exp[i\mathbf{q}\{\mathbf{r}_n(t) - \mathbf{r}_m(0)\}]\rangle h(n)h(m) =$$
$$\frac{\phi_0}{4N}\int dn dm f_{nm}(q,t)h(n)h(m) \quad (A.7)$$

where $\phi_0 = 1$ is the polymer volume fraction, $h(n) = 1$ if $n < N/2$ (i.e., for the A block), and $h(n) = -1$ if $n > N/2$ (i.e., for the B block). Here, $f_{nm}(q,t) = \int d^3 r f_{nm}(\mathbf{r},t) \exp(i\mathbf{qr})$ with $f_{nm}(\mathbf{r},t)$ being the probability density that the nth monomer of a given chain is at point $\mathbf{r}$ at the moment t under the condition that the mth link was at the origin $r = 0$ at $t = 0$. Obviously, the function $f_{nm}(\mathbf{r},t)$ must obey eq A.6, with m being a parameter. The initial ($t = 0$) condition for the function (in Fourier representation) is $f_{nm}(q,0) = \exp(-q^2\alpha^2|n - m|)$. Solving eq A.6 using the standard method of variable decoupling, one gets

$$[f_{nm}(q,t) - f_{\bar{n}m}(q,t)]/2 =$$
$$\sum_{\beta > 0} A(\beta)\psi_\beta(n)\psi_\beta(m)\exp(-\beta^2 t/t^*) \quad (A.8)$$

where $\bar{n} = N - n$, $\psi_\beta(n) = \sin[\beta(2n - N)/N]$, $A(\beta) = 2u(u^2 + \beta^2)^{-1}[1 - \sin(2\beta)/(2\beta)]^{-1}$, with the variables u, t^* defined in the main text. Here β runs over all positive values satisfying the equation $\beta/\tan\beta + u = 0$. The "bare" structure factor from eqs A.7 and A.8 is, then,

$$S_0(q,t) = \frac{N\phi_0}{2}\sum_{\beta > 0}\frac{u}{u^2 + u + \beta^2}\frac{(1 - \cos\beta)^2}{\beta^2}\exp[-\beta^2 t/t^*] \quad (A.10)$$

Hence, the susceptibility of the "ideal" system, obtained from eq A.2 is written in the form

$$\kappa_0(q,p) = \frac{N\phi_0}{4}\frac{1}{u^2 - \sigma^2}[\Psi(u,\sigma) - \Psi(u,u)] \quad (A.11)$$

where $\sigma \equiv (pt^*)^{1/2}$, $\Psi(u,\sigma) = \{2(u^2/\sigma)[1 - 1/\cosh\sigma] - \sigma\}/[\sigma + u\tanh\sigma]$, and p is the Laplace variable. Finally, the generalized susceptibility of the system with interactions between monomers is obtained from eq A.5 and is given as eq 2 in the main text.

References and Notes

(1) Sillescu, H. *Makromol. Chem., Rapid Commun.* **1984**, 5, 519; *Makromol. Chem., Rapid Commun.* **1987**, 8, 393. Green, P. F.; Doyle, B. L. *Macromolecules* **1987**, 20, 2471. Composto, R. J.; Mayer, J. W.; Kramer, E. J.; White, D. M. *Phys. Rev. Lett.* **1986**, 57, 1312. Kanetakis, J.; Fytas, G. *Macromolecules* **1989**, 22, 3452. Meier, G.; Fytas, G.; B. Momper, B.; Fleischer, G. *Macromolecules* **1993**, 26, 5310 and references therein.

(2) Erukhimovich, I. Ya.; Semenov, A. N. *Zh. Eksp. Teor. Fiz.* **1986**, 63, 259 [*Sov. Phys. JETP* **1986**, 28, 149]

(3) Akcasu, A. Z.; Benmouna, M.; Benoit, H. *Polymer* **1986**, 27, 1935. Benmouna, M.; Benoit, H.; Borsali, R.; Duval, M. *Macromolecules* **1987**, 20, 2620. Akcasu, A. Z.; Tombakoglu, M. *Macromolecules* **1990**, 23, 607. Borsali, R.; Vilgis, T. A. *J. Chem. Phys.* **1990**, 93, 3610. Borsali, R.; Fischer, E. W.; Benmouna, M. *Phys. Rev. A* **1991**, 43, 5732.

(4) Anastasiadis, S. H.; Fytas, G.; Vogt, S.; Fischer, E. W. *Phys. Rev. Lett.* **1993**, *70*, 2415. Vogt, S.; Anastasiadis, S. H.; Fytas, G.; Fischer, E. W. *Macromolecules* **1994**, *27*, 4335.

(5) Borsali, R.; Benoit, H.; Legrand, J.-F.; Duval, M.; Picot, C.; Benmouna, M.; Farago, B. *Macromolecules* **1989**, *22*, 4119. Duval, M.; Picot, C.; Benoit, H.; Borsali, R.; Benmouna, M.; Lartigue, C. *Macromolecules* **1991**, *24*, 3185.

(6) Jian, T.; Anastasiadis, S. H.; Semenov, A. N.; Fytas, G.; Adachi, K.; Kotaka, T. *Macromolecules* **1994**, *27*, 4762.

(7) Duval, M.; Haida, H.; Lingelser, J. P.; Gallot, Y. *Macromolecules* **1991**, *24*, 6867.

(8) Liu, Z.; Pan, C.; Lodge, T. P.; Stepanek, P. *Macromolecules* **1995**, *28*, 3221. Pan, C; Mauer, W; Liu, Z; Lodge, T P; Stepanek, P; von Meerwall, ED; Watanabe, H. *Macromolecules* **1995**, *28*, 1643.

(9) Fytas, G.; Anastasiadis, S. H.; Semenov, A. N. *Makromol. Chem., Macromol. Symp.* **1994**, *79*, 117. Semenov, A. N.; Fytas, G.; Anastasiadis, S. H. *Polym. Prepr.* **1994**, *35* (1), 618.

(10) T. Jian, S. H. Anastasiadis, G. Fytas, G. Fleischer, A. D. Vilesov, *Macromolecules* **1995**, *28*, 2439. Jian, T.; Fytas, G.; Anastasiadis, S. H.; Vilesov, A. D. *Polym. Mater. Sci. Eng.* **1994**, *71*, 767.

(11) Fytas, G.; Anastasiadis, S. H. In *Disorder Effects on Relaxation Processes*; Richert, R., Blumen, A., Eds.; Spinger Verlag: Berlin, 1994. Fredrickson, G. H.; Bates, F. S. *Annu. Rev. Phys. Chem.* **1996**, *26*, 503. Stepanek, P.; Lodge, T. P. In *Light Scattering*; Brown, W., Ed.; Oxford University Press: Oxford, 1996.

(12) Leibler, L. *Macromolecules* **1980**, *13*, 1602. Fredrickson, G. H.; Helfand, E. *J. Chem. Phys.* **1987**, *87*, 697. Barrat, G. L.; Fredrickson, G. H. *J. Chem. Phys.* **1991**, *95*, 1282.

(13) Bates, F. S.; Fredrickson, G. H. *Annu. Rev. Phys. Chem.* **1990**, *41*, 525. Bates, F. S. *Science* **1991**, *251*, 898.

(14) Benmouna, M.; Benoit, H. *J. Polym. Sci., Polym. Phys. Ed.* **1983**, *21*, 1227. Hong, K. M.; Noolandi, J. *Macromolecules* **1983**, *16*, 1083. Fredrickson, G. H.; Leibler, L. *Macromolecules* **1989**, *22*, 1238. Onuki, A.; Hashimoto, T. *Macromolecules* **1989**, *22*, 879. Olvera de la Cruz, M. *J. Chem. Phys.* **1989**, *90*, 1995.

(15) Hashimoto, T.; Kowasaka, K.; Shibayama, M.; Kawai, H. *Macromolecules* **1986**, *19*, 754. Hashimoto, T.; Mori, K. *Macromolecules* **1990**, *23*, 5347. Lodge, T. P.; Pan, C.; Jin, X.; Liu, Z.; Zhao, J.; Maurer, W. W.; Bates, F. S. *J. Polym. Sci., Part B: Polym. Phys.* **1995**, *33*, 2289.

(16) Boudenne, N.; Anastasiadis, S. H.; Fytas, G.; Xenidou, M.; Hadjichristidis, N.; Semenov, A. N.; Fleischer, G. *Phys. Rev. Lett.* **1996**, *77*, 506.

(17) de Gennes, P. G. *Scaling Concepts in Polymer Physics;* Cornell University Press: Ithaca, NY, 1979.

(18) de Gennes, P. G. *J. Phys.* **1981**, *42*, 735.

(19) Doi, M.; Edwards, S. F. *The Theory of Polymer Dynamics*; Oxford Science Publishers: Oxford, 1986.

(20) Jannink, G.; de Gennes, P. G. *J. Chem. Phys.* **1968**, *48*, 2260.

(21) Landau, L. D.; Lifshitz, E. M. *Statistical Physics, Part I;* Pergamon: Oxford, 1980.

(22) Brochard, F.; de Gennes, P. G. *Physica A* **1983**, *118*, 289.

(23) Graessley, W. W. *Adv. Polym. Sci.* **1974**, *16*, 1. Colby, R. H.; Rubinstein, M. *Macromolecules* **1990**, *23*, 2753.

(24) Joanny, J.-F.; Leibler, L.; Ball, R. *J. Chem. Phys.* **1984**, *81*, 4640.

(25) Schaefer, L.; Kappeler, Ch. *J. Phys. (Les Ulis, Fr.)* **1985**, *46*, 1853. Kosmas, M. *J. Phys. Lett.* **1984**, *45*, L889. Broseta, D.;

(26) de Gennes P. G. *J. Phys.* **1981**, *42*, 735.

(27) Formally eq 14b is only valid if the spatial displacement is smaller than the tube diameter; however, as one is interested in composition fluctuations on the scale $1/q$, it is possible to treat $\mathbf{R}(s(n))$ as a chain trajectory smoothed over any scale, d_{sm}, smaller than $1/q$. Equation 14b becomes formally valid if one chooses this smoothing scale in between ΔR and $1/q$: $\Delta R \ll d_{sm} \ll 1/q$.

(28) At this stage, one is now in a position to verify the only assumption that was used to derive eq 18, $\Delta R \ll 1/q$. The typical displacement of a monomer along the tube on the longest time-scale, τ_R, can be estimated as $x \sim (D_t \tau_R)^{1/2} \sim N^{1/2} b$, whereas the corresponding spatial displacement is $\Delta R \sim R_g (x/L_t)^{1/2} \sim b(NN_e)^{1/4}$. Therefore, the above treatment is valid if $1/q \gg b(NN_e)^{1/4}$. This condition is assumed below, since the experimental situation corresponds to $1/q \geq bN^{1/2}$. The dynamic length-scale $b(NN_e)^{1/4}$ has been originally considered in ref 29.

(29) Semenov, A. N. *Physica A* **1990**, *166*, 263.

(30) Bywater, S.; Toporowski, P. M. *Polymer* **1981**, *22*, 29.

(31) Jian, T.; Anastasiadis, S. H.; Fytas, G.; Adachi, K.; Kotaka, T. *Macromolecules* **1993**, *26*, 4706.

(32) Chrissopoulou, K.; Boudenne, N.; Anastasiadis, S. H.; Fytas, G.; Likhtman, A.; Semenov, A. N. In preparation

(33) Segré, P. N.; Pusey, P. N. *Phys. Rev. Lett.* **1996**, *77*, 771.

(34) L. J. Fetters, D. J. Lohse, D. Richter, T. A. Witten, A. Zirkel, *Macromolecules* **1994**, *27*, 4639.

(35) Tsenoglou, C. *J. Polym. Sci., Polym. Phys. Ed.* **1988**, *26*, 2329. Composto, R. J.; Kramer, E. J.; White, D. M. *Macromolecules* **1992**, *25*, 4167.

(36) Anastasiadis, S. H.; Chrissopoulou, K.; Fytas, G.; Appel, M.; Fleischer, G.; Adachi, K.; Gallot, Y. *Acta Polym.* **1996**, *47*, 250. Anastasiadis, S. H.; Chrissopoulou, K.; Fytas, G.; Fleischer, G.; Pispas, S.; Pitsikalis, M.; Mays, J.; Hadjichristidis, N. *Macromolecules* **1997**, *30*, 2445.

(37) Barrat, J. L.; Fredrickson, G. H. *J. Chem Phys.* **1991**, *95*, 1282. Olvera de la Cruz, M. *Phys. Rev. Lett.* **1991**, *67*, 85. Mayes, A. M.; Olvera de la Cruz, M. *J. Chem Phys.* **1991**, *95*, 4670.

(38) Fried, H.; Binder, K. *J. Chem. Phys.* **1991**, *94*, 8349.

(39) Bates, F. S.; Rosedale, J. H.; Fredrickson, G. H. *J. Chem. Phys.* **1990**, *92*, 6255. Almdal, K.; Rosedale, J. H.; Bates, F. S.; Wignall, G. D.; Fredrickson, G. H. *Phys. Rev. Lett.* **1990**, *65*, 1112.

(40) Fredrickson, G. H.; Larson, R. G. *J. Chem. Phys.* **1987**, *86*, 1553. Fredrickson, G. H.; Helfand, E. *J. Chem. Phys.* **1989**, *89*, 5890.

(41) Pincus, P. *J. Chem. Phys.* **1981**, *75*, 1996. Binder, K. *J. Chem. Phys.* **1983**, *79*, 6387. Kawasaki, K.; Sekimoto, K. *Macromolecules* **1989**, *22*, 3063.

(42) Chrissopoulou, K.; Anastasiadis, S. H.; Fytas, G.; Xenidou, M.; Hadjichristidis, N. In preparation

(43) Richter, D.; Willmer, L.; Zirkel, A.; Farago, B.; Fetters, L. J.; Kuang, J. S. *Macromolecules* **1994**, *27*, 7437.

(44) Anastasiadis, S. H.; Fleischer, G.; Fytas, G.; Semenov, A. N.; Kärger, J.; Xenidou, M.; Hadjichristidis, N. *Phys. Rev. Lett.*, submitted.